



# Global maps of twenty-first century forest carbon fluxes

Nancy L. Harris<sup>1</sup>✉, David A. Gibbs<sup>1</sup>, Alessandro Vaccini<sup>2,10</sup>, Richard A. Birdsey<sup>2</sup>, Sytze de Bruin<sup>1</sup><sup>3</sup>, Mary Farina<sup>2,11</sup>, Lola Fatoyinbo<sup>4</sup>, Matthew C. Hansen<sup>1</sup><sup>5</sup>, Martin Herold<sup>1</sup><sup>3</sup>, Richard A. Houghton<sup>2</sup>, Peter V. Potapov<sup>1</sup><sup>5</sup>, Daniela Requena Suarez<sup>1</sup><sup>3</sup>, Rosa M. Roman-Cuesta<sup>6</sup>, Sassan S. Saatchi<sup>7,8</sup>, Christy M. Slay<sup>1</sup><sup>9</sup>, Svetlana A. Turubanova<sup>5</sup> and Alexandra Tyukavina<sup>5</sup>

**Managing forests for climate change mitigation requires action by diverse stakeholders undertaking different activities with overlapping objectives and spatial impacts. To date, several forest carbon monitoring systems have been developed for different regions using various data, methods and assumptions, making it difficult to evaluate mitigation performance consistently across scales. Here, we integrate ground and Earth observation data to map annual forest-related greenhouse gas emissions and removals globally at a spatial resolution of 30 m over the years 2001–2019. We estimate that global forests were a net carbon sink of  $-7.6 \pm 49 \text{ GtCO}_2\text{e yr}^{-1}$ , reflecting a balance between gross carbon removals ( $-15.6 \pm 49 \text{ GtCO}_2\text{e yr}^{-1}$ ) and gross emissions from deforestation and other disturbances ( $8.1 \pm 2.5 \text{ GtCO}_2\text{e yr}^{-1}$ ). The geospatial monitoring framework introduced here supports climate policy development by promoting alignment and transparency in setting priorities and tracking collective progress towards forest-specific climate mitigation goals with both local detail and global consistency.**

Climate change must be addressed by various actors including scientists, policymakers, companies, investors and civil society, all of whom operate under different mandates and capabilities. Both IPCC reports<sup>1,2</sup> and the Paris Agreement<sup>3</sup> recognize that climate change mitigation goals cannot be achieved without a substantial contribution from forests but monitoring the extent to which forests impact atmospheric greenhouse gas (GHG) concentrations is challenging. Opposing fluxes (emissions from sources (+) and removals by sinks (-)) occur simultaneously within regions on the basis of where and when disturbance and management take place, interannual variability can be high and land-use patterns are more dynamic and operate on finer spatiotemporal scales than reflected in most global models<sup>4</sup>. Furthermore, ability to distinguish anthropogenic from non-anthropogenic effects is limited on the basis of direct observation<sup>2</sup> and most estimation methods offer few details about where, when and why forest fluxes occur. Yet understanding the magnitude, drivers and spatial distribution of carbon fluxes across the world's forests, and how they can be managed both to reduce emissions and enhance removals, is increasingly important for climate policy and the various actors developing nature-based solutions<sup>5</sup>.

Current estimates of terrestrial GHG fluxes vary with respect to scope, definitions, assumptions and level of transparency and completeness. At the global scale, the net annual carbon dioxide (CO<sub>2</sub>) flux from anthropogenic land-use and land-cover change—driven mainly by tropical deforestation—is estimated in IPCC reports<sup>1,2</sup> and the Global Carbon Project<sup>6</sup> by a bookkeeping model<sup>7,8</sup> or by dynamic global vegetation models<sup>6</sup>. The remaining

non-anthropogenic sink of atmospheric carbon on land—predominantly forests<sup>9</sup>—is then inferred as the residual of the other terms of the global carbon budget<sup>1</sup>. Another approach compiles national GHG inventories (GHGIs), which reflect methodologies developed by the IPCC and agreed to under the United Nations Framework Convention on Climate Change<sup>10,11</sup>. The quality, methodological complexity and sources of data used by each country vary, as do the completeness and frequency of reporting. These approaches produce dissimilar global net forest fluxes; GHGI estimates compiled from country reports are 4.3 GtCO<sub>2</sub> yr<sup>-1</sup> lower than global estimates from models summarized in IPCC reports—a discrepancy larger than the total annual emissions of India, the world's third highest emitter<sup>12</sup>. A substantial part of this discrepancy (about 3.2 GtCO<sub>2</sub> yr<sup>-1</sup>) can be explained by conceptual differences in what is counted in the anthropogenic forest sink. Beyond this large disparity in global estimates, data and methodological mismatches also exist across project, subnational and national forest GHG measurement systems, leading to complications around integrating smaller-scale activities into larger national or subnational monitoring programmes<sup>13</sup> and around the potential international transfer of forest-related emission reductions versus those achieved as part of a country's own nationally determined contribution<sup>14</sup>. In sum, the complexity and lack of spatial detail in GHG measurement systems contributes to confusion about the role forests play in climate mitigation targets and discourages the transformational action and ambition needed in the forest sector to achieve global climate goals.

Here, we introduce a transparent, independent and spatially explicit global system for monitoring the collective impact of

<sup>1</sup>World Resources Institute, Washington DC, USA. <sup>2</sup>Woodwell Climate Research Center, Falmouth, MA, USA. <sup>3</sup>Laboratory of Geo-Information Science and Remote Sensing, Wageningen University and Research, Wageningen, the Netherlands. <sup>4</sup>Biospheric Sciences Laboratory, NASA Goddard Space Flight Center, Greenbelt, MD, USA. <sup>5</sup>Department of Geographical Sciences, University of Maryland, College Park, MD, USA. <sup>6</sup>Center for International Forestry Research (CIFOR), Bogor, Indonesia. <sup>7</sup>Jet Propulsion Laboratory, California Institute of Technology, Pasadena, CA, USA. <sup>8</sup>Institute of Environment, University of California, Los Angeles, CA, USA. <sup>9</sup>The Sustainability Consortium, University of Arkansas, Fayetteville, AR, USA. <sup>10</sup>Present address: Department of Earth and Environment, Boston University, Boston, MA, USA. <sup>11</sup>Present address: Department of Land Resources and Environmental Sciences, Montana State University, Bozeman, MT, USA. ✉e-mail: [nharris@wri.org](mailto:nharris@wri.org)

forest-related climate policies implemented by diverse actors across multiple scales. We complement existing global forest carbon flux estimation approaches of large area vegetation models and aggregation of national inventories with a third approach that capitalizes on recent advances in Earth observation. Using recently revised IPCC guidelines as a methodological framework<sup>10,11</sup>, we separately map GHG emissions (sources) and carbon dioxide removals (sinks) from global forest lands at 30-m resolution between 2001 and 2019 (Methods). Areas of forest extent, loss and gain from the Global Forest Change product of Hansen et al.<sup>15</sup> form the basis of the activity data. By co-locating activity data with spatially explicit emission and removal factors developed from integrating ground and Earth observation monitoring data on land use and management type, forest type, forest age class, fire history and biomass and soil carbon stocks, we separately map gross annual carbon removals occurring within natural, seminatural and planted forests and gross annual emissions arising from five dominant drivers of forest disturbance. We then map the difference between gross emissions (+) and gross removals (−) as the net annual forest-related GHG flux, which may be positive or negative in an area depending on the balance of gross fluxes. Tracking gross emissions and removals separately, rather than solely the net balance between the two, underscores the dual role of forests as sources and sinks in the global carbon cycle and facilitates more complete and transparent accounting of the individual pathways involved in forest-based mitigation (reducing emissions and increasing removals).

### Global distribution of forest emissions and removals

Between 2001 and 2019, deforestation and other satellite-observed forest disturbances resulted in global gross GHG emissions of  $8.1 \pm 2.5 \text{ GtCO}_2\text{e yr}^{-1}$  (mean  $\pm$  s.d.). Carbon dioxide ( $\text{CO}_2$ ) was the dominant GHG; methane ( $\text{CH}_4$ ) and nitrous oxide ( $\text{N}_2\text{O}$ ) emissions from stand-replacing forest fires and drainage of organic soils in deforested areas accounted for 1.1% of gross emissions ( $0.088 \text{ GtCO}_2\text{e yr}^{-1}$ ). Over the same period, gross carbon removals by forest ecosystems were  $-15.6 \pm 49 \text{ GtCO}_2\text{e yr}^{-1}$ . Taken together, the balance of these opposing fluxes (gross emissions and gross removals) yields a global net GHG forest sink of  $-7.6 \pm 49 \text{ GtCO}_2\text{e yr}^{-1}$  (Table 1 and Fig. 1). The large uncertainties in global gross removals and net flux are almost entirely due to extremely high uncertainty in removal factors from the IPCC Guidelines<sup>11</sup> applied to old secondary temperate forests outside the United States and Europe (Supplementary Table 1).

Tropical and subtropical forests contributed the most to global gross forest fluxes, accounting for 78% of gross emissions ( $6.3 \pm 2.4 \text{ GtCO}_2\text{e yr}^{-1}$ ) and 55% of gross removals ( $-8.6 \pm 7.6 \text{ GtCO}_2\text{e yr}^{-1}$ ) (Table 1). While these forests removed more atmospheric carbon than temperate and boreal forests on a gross basis ( $-8.6$  versus  $-4.4$  and  $-2.5 \text{ GtCO}_2\text{e yr}^{-1}$ , respectively), tropical and subtropical forests contributed just 30% to the global net carbon sink; about two-thirds of the global net sink was in temperate (47%) and boreal (21%) forests, resulting from substantially lower gross emissions there than in the subtropics and tropics (0.87 and  $0.88 \text{ GtCO}_2\text{e yr}^{-1}$ , respectively).

Just six large forested countries (Brazil, Canada, China, Democratic Republic of the Congo, Russia and the United States) accounted for 51% of global gross emissions, 56% of global gross removals and 60% of net flux. Forests in nearly all countries were net carbon negative, that is, gross carbon removals from established and regrowing forests exceeded gross emissions from land-use change and other forest disturbances. The main exceptions were in Indonesia, Malaysia, Cambodia and Laos, where annual gross emissions across these countries ( $1.36 \text{ GtCO}_2\text{e yr}^{-1}$ ), including peat drainage and burning ( $0.14 \text{ GtCO}_2\text{e yr}^{-1}$ ), exceeded gross removals ( $-0.83 \text{ GtCO}_2\text{e yr}^{-1}$ ) (Fig. 2). Globally, 72% of gross removals were concentrated in older ( $>20$  yr) secondary natural and seminatural

forests, 12% in tropical primary forests, 10% in plantations, 3.5% in young ( $<20$  yr) forest regrowth, 1.3% in mangroves and 0.34% in boreal and temperate intact forest landscapes (Table 1).

### Fluxes for specific localities and drivers of forest change

Our analysis enables consistent evaluation of forest GHG dynamics across scales and in custom geographies beyond national or climate domain boundaries (Fig. 1). For example, ~27% of the global net forest GHG sink occurred within protected areas<sup>16</sup>. Forests in the Brazilian Amazon were a net carbon source of  $0.22 \text{ GtCO}_2\text{e yr}^{-1}$  between 2001 and 2019, whereas forests across the larger Amazon River basin—encompassing 514 Mha of forests across nine countries—were a net carbon sink of  $-0.10 \text{ GtCO}_2\text{e yr}^{-1}$ . Although smaller in extent than the Amazon, the net sink in forests of Africa's Congo River basin (298 Mha) was approximately six times stronger ( $-0.61 \text{ GtCO}_2\text{e yr}^{-1}$ ), reflecting nearly identical gross removals ( $-1.1$  versus  $-1.2 \text{ GtCO}_2\text{e yr}^{-1}$ ) but gross emissions that were half those of the Amazon basin (0.53 versus  $1.1 \text{ GtCO}_2\text{e yr}^{-1}$ ).

From overlaying forest GHG flux maps in Fig. 1 with a global map of dominant drivers of forest disturbance<sup>17</sup>, we estimate that commodity-driven deforestation was the largest source of gross forest-related emissions between 2001 and 2019 ( $2.8 \text{ GtCO}_2\text{e yr}^{-1}$ ) and occurred primarily in the rainforests of South America and Southeast Asia. Forests in shifting agriculture landscapes, a dominant land use in the tropics characterized by cycles of small-scale forest clearing of both primary and secondary forests followed by secondary regrowth, contributed another  $2.1 \text{ GtCO}_2\text{e yr}^{-1}$  to gross emissions and  $-3.3 \text{ GtCO}_2\text{e yr}^{-1}$  to gross removals, leading to a net sink in these areas of  $-1.2 \text{ GtCO}_2\text{e yr}^{-1}$ . Gross emissions from stand-replacing forest fires, occurring primarily in temperate and boreal forests, averaged  $0.69 \text{ GtCO}_2\text{e yr}^{-1}$ . Forestry-dominated landscapes, comprised of both plantations and natural and seminatural forests, were a net sink of  $-3.3 \text{ GtCO}_2\text{e yr}^{-1}$  between 2001 and 2019. This reflects  $2.4 \text{ GtCO}_2\text{e yr}^{-1}$  of gross emissions from harvest offset by  $-5.5 \text{ GtCO}_2\text{e yr}^{-1}$  of gross removals from forest management and regeneration and  $-0.16 \text{ GtCO}_2\text{e yr}^{-1}$  of increased carbon storage in harvested wood products.

### A flexible data integration framework

The IPCC Guidelines used as the overarching methodological framework in this analysis<sup>10,11</sup> provide three tiers of methods, parameters and data sources for GHG flux estimation, where progression from Tier 1 to Tier 3 generally results in more accurate and precise estimates at the expense of more analytical complexity and larger data requirements. For forests, Tier 3 estimates are characterized by the incorporation of repeated, country-specific measurements over time but the land-use definitions and the spatial scale of data sources chosen can impact the resulting estimates. Therefore, in addition to estimating uncertainty in GHG estimates within geographies for which information was available to do so (climate domains), we also conducted sensitivity analyses to demonstrate how estimates change as data inputs and model assumptions are varied within our spatial data integration framework (Supplementary Information). At the global scale, GHG flux estimates were relatively insensitive to changes in model assumptions; estimates for most pixels changed less than 15% in either direction and sources stayed sources while sinks stayed sinks.

However, estimates were more affected by changes in data sources, particularly at local scales. For example, replacing the global 30-m biomass map developed in this study as the basis of emission factors (Extended Data Fig. 1) with a coarser (1-km) resolution biomass map produced by Saatchi et al.<sup>18</sup> for the tropics produced 12% lower gross GHG emissions there than our original estimate. Replacing the 30-m annual tree cover loss data from Hansen et al.<sup>15</sup> in the Brazilian Amazon with annual forest loss data from Brazil's national forest monitoring system<sup>19</sup>, which

**Table 1 | Forest-related GHG fluxes by climate domain and forest type**

Climate domain	Forest type	Forest extent 2000 (Mha)	GtCO <sub>2</sub> eyr <sup>-1</sup> , 2001–2019					
			Gross emissions	Percentage of global total	Gross removals	Percentage of global total	Net GHG flux	Percentage of global total <sup>d</sup>
Boreal	Primary <sup>a</sup>	38	0.26	3.2	-0.044	0.28	0.22	
	Old secondary (>20 yr)	1,030	0.60	7.4	-2.4	15	-1.8	
	Young secondary ( $\leq$ 20 yr)	22	0.015	0.19	-0.037	0.24	-0.022	
	Plantations/tree crops <sup>b</sup>	0.21	0.000056	0.00070	-0.0027	0.017	-0.0027	
<b>Total boreal</b>		<b>1,090</b>	<b>0.88<math>\pm</math>0.42</b>	<b>11</b>	<b>-2.5<math>\pm</math>0.96</b>	<b>16</b>	<b>-1.6<math>\pm</math>1.1</b>	<b>21</b>
Temperate	Primary <sup>a</sup>	2.3	0.036	0.45	-0.0092	0.059	0.027	
	Old secondary (>20 yr)	560	0.71	8.8	-4.2	27	-3.5	
	Young secondary ( $\leq$ 20 yr)	16	0.049	0.60	-0.039	0.25	0.0092	
	Plantations/tree crops <sup>b</sup>	12	0.071	0.88	-0.14	0.92	-0.073	
<b>Total temperate</b>		<b>590</b>	<b>0.87<math>\pm</math>0.60</b>	<b>11</b>	<b>-4.4<math>\pm</math>48</b>	<b>28</b>	<b>-3.6<math>\pm</math>48</b>	<b>47</b>
Subtropical	Primary <sup>a</sup>	3.6	0.0062	0.076	-0.0058	0.037	0.00035	
	Old secondary (>20 yr)	270	0.46	5.7	-0.84	5.4	-0.38	
	Young secondary ( $\leq$ 20 yr)	13	0.11	1.3	-0.067	0.43	0.040	
	Plantations/tree crops <sup>c</sup>	54	0.40	5.0	-0.71	4.6	-0.31	
	Mangroves	0.070	0.000066	0.00082	-0.0040	0.026	-0.0040	
<b>Total subtropical</b>		<b>340</b>	<b>1.0<math>\pm</math>0.59</b>	<b>12</b>	<b>-1.6<math>\pm</math>0.56</b>	<b>10</b>	<b>-0.65<math>\pm</math>0.81</b>	<b>8.6</b>
Tropical	Primary <sup>a</sup>	1,010	1.8	22	-1.9	12	-0.12	
	Old secondary (>20 yr)	880	1.9	23	-3.8	24	-1.9	
	Young secondary ( $\leq$ 20 yr)	47	0.76	9.5	-0.40	2.5	0.37	
	Plantations/tree crops <sup>c</sup>	47	0.89	11	-0.73	4.7	0.16	
	Mangroves	7.2	0.010	0.12	-0.16	1.0	-0.15	
<b>Total tropical</b>		<b>1,990</b>	<b>5.3<math>\pm</math>2.4</b>	<b>66</b>	<b>-7.0<math>\pm</math>7.6</b>	<b>45</b>	<b>-1.7<math>\pm</math>8.0</b>	<b>22</b>
Global	Primary	1,060	2.1	26	-2.0	13	0.13	
	Old secondary (>20 yr)	2,750	3.7	45	-11	72	-7.7	
	Young secondary ( $\leq$ 20 yr)	99	0.9	12	-0.54	3.5	0.39	
	Plantations/tree crops	113	1.4	17	-1.6	10	-0.23	
	Mangroves	8.7	0.012	0.14	-0.20	1.3	-0.19	
<b>Total global</b>		<b>4,029</b>	<b>8.1<math>\pm</math>2.5</b>	<b>100</b>	<b>-16<math>\pm</math>49</b>	<b>100</b>	<b>-7.6<math>\pm</math>49</b>	<b>100</b>

Average annual gross GHG emissions, gross GHG removals and net GHG fluxes across global forest lands between 2001 and 2019. Estimates reflect forest ecosystem fluxes only; harvested wood products are excluded. Uncertainties are expressed as s.d. Large uncertainties in net flux estimates should be interpreted with caution; s.d. are very large relative to the estimates in part because net flux estimates reflect the sum of negative (removals) and positive (emissions) terms, complicating the combination of their error terms.<sup>a</sup>The extent of primary forests was delineated differently for tropical and extratropical regions (Methods).<sup>b</sup>Fluxes occurring within seminatural managed forests are reported in the relevant secondary forest category (old or young).<sup>c</sup>Fluxes reported in the plantation/tree crop category include those associated with conversion of natural forests to plantations or tree crops (for example, oil palm) over the 2001–2019 analysis period.<sup>d</sup>Calculating percentages of net flux by forest type is complicated by the mixture of sources and sinks among forest types, and is thus omitted.

excludes deforestation events smaller than 6.25 ha, reduced average gross emissions there from 1.1 to 0.74 GtCO<sub>2</sub>eyr<sup>-1</sup>. This difference arises from increased detection of emissions from small forest clearings. Both examples highlight the value of our spatially detailed approach in capturing more changes and larger fluxes occurring at small scales where many human-induced forest changes are occurring. In the United States, replacing Tier 3 removal factors estimated specifically for US forest types and age classes from repeated inventory measurements with generalized Tier 1 defaults from the updated IPCC Guidelines<sup>11</sup> led to a 38% stronger net carbon sink there than the original estimate. (See Supplementary Table 2 and Extended Data Figs. 2–8 for additional examples.) These analyses quantitatively and spatially demonstrate tradeoffs between globally consistent analyses and locally derived values that are difficult to aggregate globally and may not be available or comparable across regions. The flexible spatial data integration framework introduced here enhances science-policy coordination by providing a more

systematic, structured, transparent and verifiable system for exploring differences in data, assumptions and resulting estimates than what has been available previously.

### Forest fluxes in the global carbon budget

Our results are not directly comparable to other global estimates because other estimates typically reflect all terrestrial fluxes (versus forests only), report only net fluxes (versus gross and net fluxes), include only CO<sub>2</sub> (versus all relevant GHGs) and make assumptions to partition between anthropogenic and non-anthropogenic net fluxes<sup>2,12</sup>. While the spatial, observation-based framework introduced here permits estimation of fluxes for any forest definition and the inclusion (or exclusion) of any geographic area of interest, it cannot distinguish between anthropogenic versus non-anthropogenic effects or between managed versus unmanaged land until the requisite spatial data become available to differentiate them<sup>20</sup>. When considering only CO<sub>2</sub> fluxes to improve comparability with the

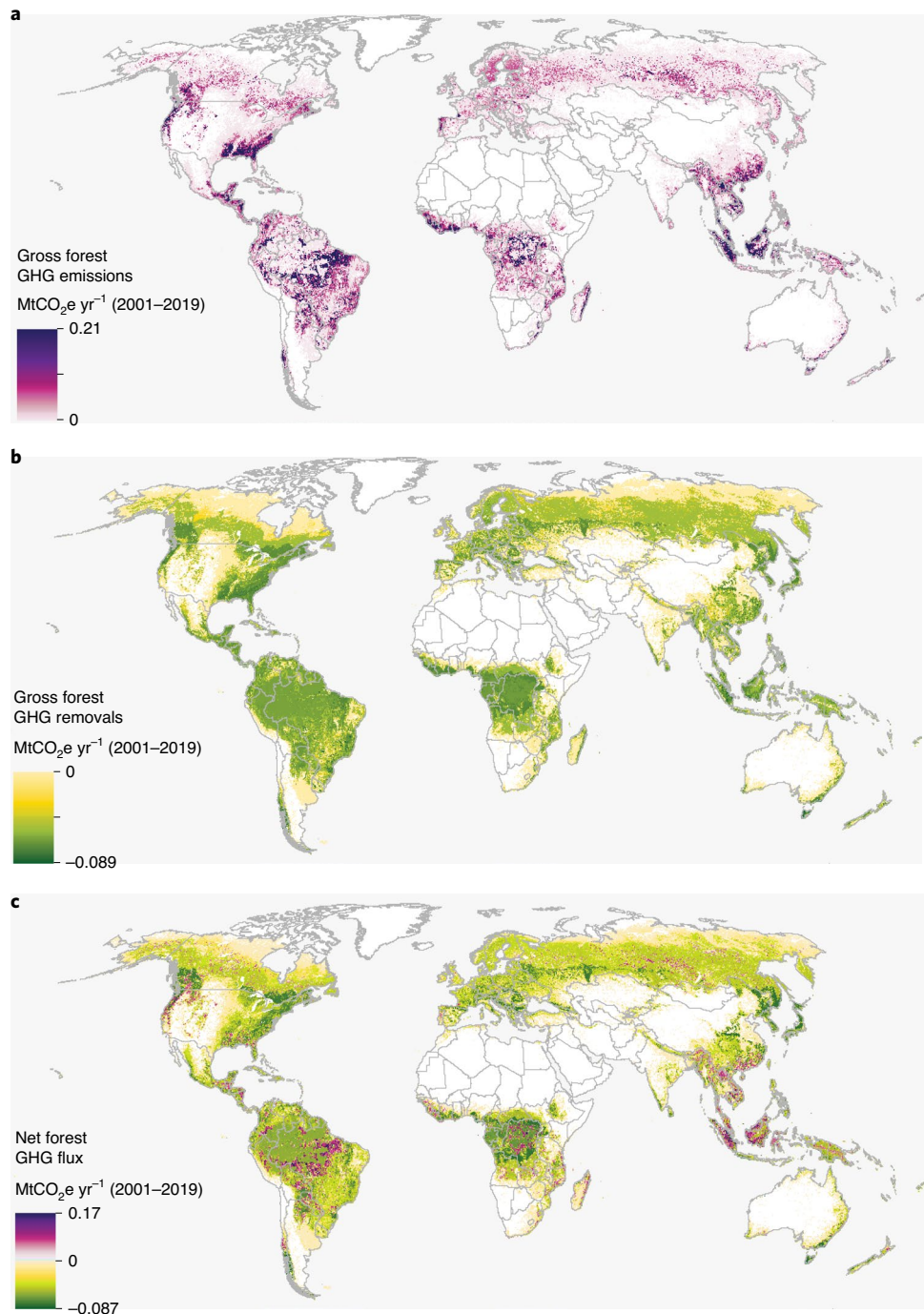


**Fig. 1 | Forest-related GHG fluxes (annual average, 2001–2019).** **a**, Gross annual GHG emissions. **b**, Gross annual GHG removals. **c**, Net annual GHG flux. For display purposes, maps have been resampled from the 30-m observation scale to a 0.04° geographic grid. Values in the legend reflect the average annual GHG flux from all forest dynamics occurring within a grid cell, including emissions from all observed disturbances and removals from both forest regrowth after disturbance as well as removals occurring in undisturbed forests.

Global Carbon Budget, we estimate a larger net CO<sub>2</sub> sink by forest ecosystems ( $-7.8 \text{ GtCO}_2 \text{ yr}^{-1}$ ) than its estimate of  $-5.2 \text{ GtCO}_2 \text{ yr}^{-1}$  for all terrestrial fluxes over the same time period<sup>6</sup>. One potential reason for this difference is that our model underestimates gross forest-related emissions due to the exclusion of forest disturbances that go undetected and unquantified in the medium resolution satellite observations that underpin our analysis. Gross emissions from tropical forest degradation have been estimated as  $2.1 \text{ GtCO}_2 \text{ yr}^{-1}$ , with selective logging, fuelwood harvest and non-stand-replacing

fires accounting for 53, 30 and 17% of the total, respectively<sup>21</sup>. Adding this (non-spatial) estimate of gross degradation emissions to our satellite-based gross carbon emission and removal estimates occurring within forest ecosystems, as well as  $-0.16 \text{ GtCO}_2 \text{ yr}^{-1}$  of net removals in harvested wood products, yields a revised net forest-atmosphere CO<sub>2</sub> flux of  $-5.8 \text{ GtCO}_2 \text{ yr}^{-1}$  (Table 2). Taken together, these estimates of gross removals ( $-15.6 \text{ GtCO}_2 \text{ yr}^{-1}$ ) and gross emissions related to forests (including degradation:  $10 \text{ GtCO}_2 \text{ yr}^{-1}$ ) appear to nearly balance the global carbon budget

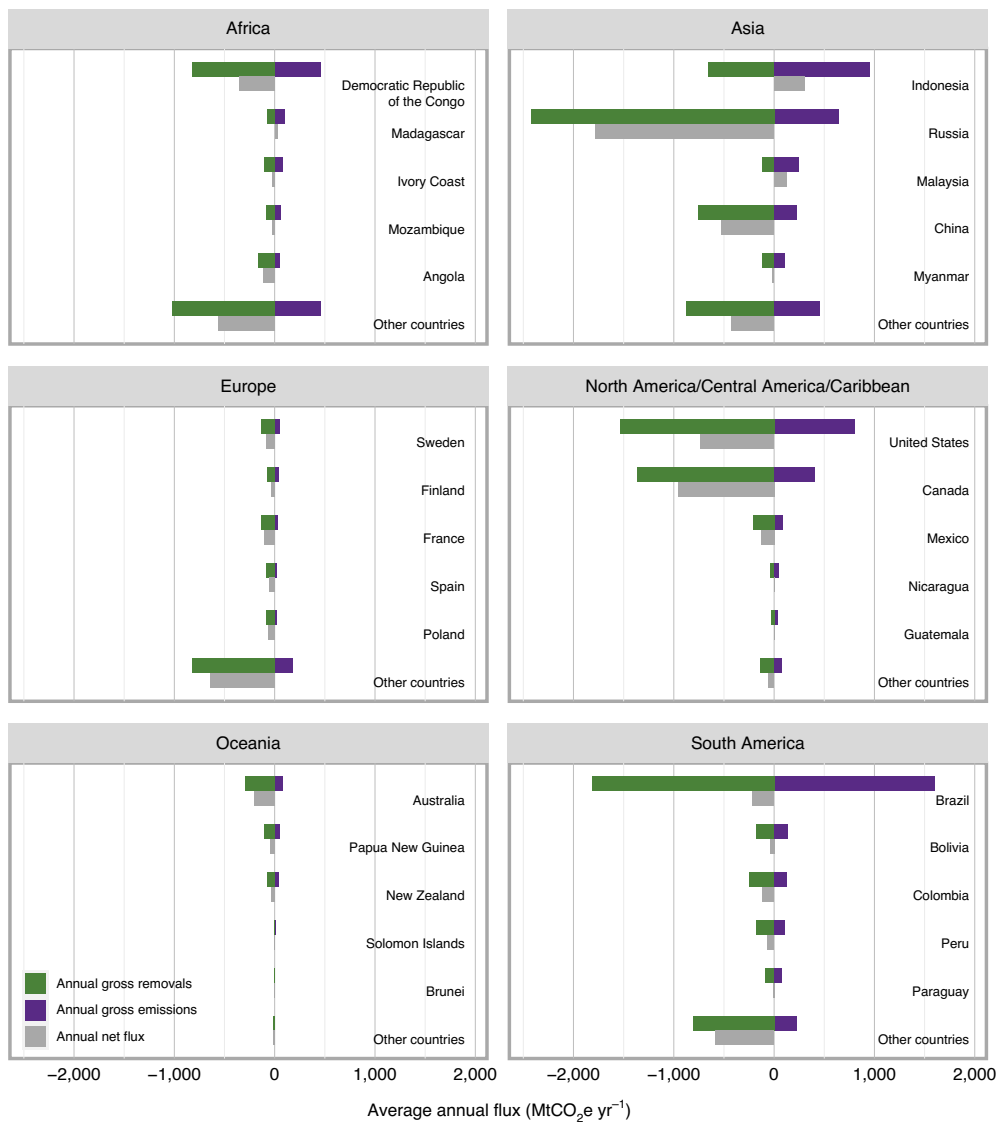


**Fig. 2 | Gross and net GHG fluxes from forests by region (annual average, 2001–2019).** Net forest-related fluxes (grey bars) are shown with their two component gross fluxes: gross emissions from land-use change and other forest disturbances (purple) and gross removals occurring in undisturbed forests as well as removals from forest regrowth after disturbance (green). The top five countries per region are ranked high to low on the basis of gross emissions, with all other countries in the region grouped into ‘other countries’.

(Table 2) but other important fluxes are omitted from our analysis such as those occurring within grasslands, semi-arid savannas and shrublands<sup>22</sup> (due to the 30% per 5 m of tree cover definition used in our analysis), non-stand-replacing fires<sup>23</sup>, degradation outside the tropics and other terrestrial fluxes not previously included in any global budget to date<sup>24</sup>. We include Table 2 to highlight how our gross estimates of forest-related fluxes fit within the context of the global carbon budget but our research is geared towards highlighting forest emission and removal hotspots for policy-relevant applications and stakeholders (Fig. 1), not towards producing a comprehensive and precise accounting of the full terrestrial carbon budget.

### Limitations and future improvements

All forest monitoring systems reflect a balance between data availability, scale of applicability, measurement costs, reducing uncertainties and other constraints. Given the urgency of addressing climate change, the time and costs required to develop monitoring systems that reduce uncertainties as far as practicable<sup>25</sup> must be balanced

against the potential benefits of publicly accessible, operational and fit-for-purpose systems that provide enough spatial detail to incentivize real, near-term and sustained investment in nature-based climate solutions on the ground. In this study, we combined publicly available data into a global monitoring framework that generates consistent information on forest carbon fluxes cost-effectively over large spatial scales. However, this approach encounters limitations that should be addressed as research progresses.

First, the global forest change data used as the basis of activity data in our analysis are spatially detailed but contain temporal inconsistencies. While the forest loss product is updated annually through 2019, gain has not been updated past 2012 and represents a cumulative total (2000–2012). Therefore, although gross emissions can be estimated annually (Extended Data Fig. 9), estimating annual trends in gross removals and net flux is limited by a lack of a consistent time series on forest regrowth. Globally, GHG flux estimates were relatively insensitive to this limitation; we estimate that expansion of forest extent observed after 2000 accounted for less than 5% of global gross carbon removals, with the vast majority occurring

**Table 2 | Comparison of results from this study to the Global Carbon Project, 2001–2018**

Global carbon budget, 2001–2018 (GtCO <sub>2</sub> yr <sup>-1</sup> )			
Global Carbon Project	This study		
Sources			
Fossil fuel and cement	32.0	Fossil fuel and cement	32.0
Land-use change (net, anthropogenic) <sup>a</sup>	5.3	Forests (gross, all observed disturbances) <sup>b</sup>	7.9
		Forests (gross, unobserved emission sources) <sup>c</sup>	2.1
<b>Total sources</b>	<b>37.3</b>		<b>42.0</b>
Sinks			
Atmosphere	16.9	Atmosphere	16.9
Ocean	8.7	Ocean	8.7
Terrestrial (net, non-anthropogenic) <sup>d</sup>	10.5	Forests (gross, all forests) <sup>e</sup>	15.6
		Harvested wood products	0.16
<b>Total sinks</b>	<b>36.1</b>		<b>41.4</b>
Land (net, all land)	-5.2	Forests (net, all forests) <sup>f</sup>	-5.8
Budget imbalance <sup>g</sup>	1.2		0.6

Estimates from the Global Carbon Project (GCP)<sup>10</sup> and this study are not directly comparable due to differences in scope (all land versus forests, respectively), data, methodologies and reporting structure. In GCP reporting, land-use change emissions (sources) reflect the net balance between anthropogenic emissions (+) and removals (-), thus the net emission estimate is lower than gross emissions reported in this study. Similarly, gross removals reported in this study reflect removals across all forest lands, including removals implicit (but unreported) in the net land-use change estimate of GCP. <sup>10</sup>Estimates only net direct anthropogenic effects, including deforestation, afforestation/reforestation and wood harvest. Gross fluxes higher but not reported. <sup>a</sup>Gross emissions from all forest disturbances (anthropogenic and non-anthropogenic) observed from Landsat data. Estimate includes CO<sub>2</sub> only for comparability with GCP; non-CO<sub>2</sub> emissions are 0.086 GtCO<sub>2</sub> yr<sup>-1</sup>. <sup>b</sup>Gross emissions from forest degradation in 74 developing countries covering 2.2 billion hectares of forest, from Pearson et al.<sup>21</sup>. <sup>c</sup>In IPCC's Fifth Assessment Report, calculated as the residual of all other terms in the carbon budget. <sup>d</sup>Gross removals from all forest processes (direct, indirect and natural). <sup>e</sup>Calculated as the net balance between gross forest ecosystem emissions and removals (7.9+21.15.6 GtCO<sub>2</sub> yr<sup>-1</sup>) plus an additional net removal of -0.16 GtCO<sub>2</sub> yr<sup>-1</sup> in harvested wood products. <sup>f</sup>Budget imbalance is the difference between total sources and total sinks.

instead in forests established before 2000. However, accurate monitoring of the timing of recent regrowth becomes more important in local contexts where rapid forest loss/gain dynamics are occurring, such as in plantations with short rotation cycles and other dynamic areas dominated by intensive forestry or short-fallow shifting cultivation systems (Extended Data Fig. 5). Temporal inconsistencies are also present within the global loss product; one algorithm covers years 2001–2010 and another covers 2011–2019, with later years of loss likely to be more sensitive to changes related to small-scale agriculture, fires and other forms of forest degradation. For these reasons, we report only long-term averages and not annual trends in forest GHG fluxes. A forthcoming ‘version 2’ global tree cover loss product and an improved global gain product, already piloted for the lower Mekong region of Southeast Asia<sup>26</sup>, will improve temporal consistency. Incorporating these improvements into the forest GHG flux model will more accurately capture interannual variability in emissions and removals over time and will thus provide a consistent basis for more temporally detailed monitoring of the long-term net impact of forests on atmospheric GHGs<sup>27</sup>.

Second, information is currently lacking to develop globally consistent and spatially detailed maps of forest carbon removals. In our analysis, uncertainty in gross removals is substantially higher than uncertainty in gross emissions, driven primarily by high uncertainty in removal factors for established forests in temperate regions (Table 1 and Supplementary Table 1). Through the integration of

ground and Earth observation data, several biomass and soil carbon maps have been developed that inform spatially explicit emission factors. However, accurate and precise estimation of forest carbon removal factors requires information derived from long-term forest inventories applied consistently and repeatedly through time across different forest types and age classes. For many of the world’s forests, this information does not exist<sup>28</sup>. Many developing countries have not completed their first forest inventory, let alone repeated inventories. Efforts to combine georeferenced plot networks with other spatially explicit data inputs to create maps over large scales of forest carbon accumulation rates over time, similar to what has been done to develop biomass density maps at a single point in time, have begun but are still in their infancy<sup>29</sup>. We therefore applied removal factors using a stratification approach, where each forest pixel is assigned a removal factor on the basis of its geographic region, forest type and age class (Methods). Removal factors reflect both ecological forest dynamics (tree growth, mortality and recruitment through natural regeneration) and indirect effects (long-term increases in atmospheric CO<sub>2</sub> concentrations and temperature, nutrient fertilization). Going forward, new satellite missions such as GEDI, ICESAT-2 and BIOMASS will provide repeated measurements of forest height and biomass over time that should improve understanding of spatial variation in rates of carbon removal across heterogeneous forest landscapes.

The global forest carbon monitoring framework introduced here, and the main improvements identified above, allow for efficient prioritization and evaluation of how data updates and improvements influence GHG flux estimates and their uncertainties. As satellite- and ground-based forest monitoring improve, so too will the associated forest GHG flux estimates.

## Conclusions

Our analysis reinforces the need to reduce gross emissions from tropical deforestation as a climate change mitigation strategy, while also highlighting the substantial but often underappreciated contribution of intact primary and older secondary forests to carbon dioxide removals. Quantifying gross emissions and removals separately and consistently across all forest lands—and producing maps in addition to tabular statistics—improves transparency in the accounting of factors and geographies contributing to the global net forest GHG flux. It also provides a framework to integrate new and improved data sources over time. Governments interested in spatially prioritizing implementation and tracking of national and subnational forest mitigation targets can increasingly make use of such data. Non-government actors, such as companies aiming to reduce emissions from deforestation associated with commodity supply chains and emerging market mechanisms considering the inclusion of forests for carbon offset programs, could benefit from a globally consistent and spatially explicit forest monitoring system developed using the same internationally accepted methods as national governments use but based on independent observations and with GHG estimates that can be linked to individual actions and generated at scales relevant to diverse climate-related policies, programmes and stakeholders.

The goals of the Paris Agreement—primarily, net zero anthropogenic emissions in the second half of this century—create an imperative to track forest-related emissions and removals transparently and at scales that link more closely to mitigation activities on the ground. As the capacity of national governments to collect, process and analyse data continues to improve, the global forest carbon monitoring framework introduced here can help to enhance transparency, inform forest-related climate policy and implementation initiatives, underpin independent technical assessments, reconcile differences between national reports and scientific studies, and provide a more consistent and comparable basis for tracking progress at local scales and for assessing atmospheric

impacts of global forest change under the Paris Agreement's forthcoming Global Stocktake<sup>30</sup>.

## Online content

Any methods, additional references, Nature Research reporting summaries, source data, extended data, supplementary information, acknowledgements, peer review information; details of author contributions and competing interests; and statements of data and code availability are available at <https://doi.org/10.1038/s41558-020-00976-6>.

Received: 15 May 2020; Accepted: 3 December 2020;

Published online: 21 January 2021

## References

1. IPCC *Climate Change 2014: Synthesis Report* (eds Core Writing Team, Pachauri, R. K. & Meyer L. A.) (IPCC, 2014).
2. IPCC *Special Report on Climate Change, Desertification, Land Degradation, Sustainable Land Management, Food Security, and Greenhouse Gas Fluxes in Terrestrial Ecosystems* (IPCC, 2019).
3. *Adoption of the Paris Agreement FCCC/CP/2015/10/Add.1* (UNFCCC, 2015).
4. Klein Goldewijk, K., Beusen, A., Doelman, J. & Stehfest, E. New anthropogenic land use estimates for the Holocene: HYDE 3.2. *Earth Syst. Sci. Data* **9**, 927–953 (2017).
5. Griscom, B. W. et al. National mitigation potential from natural climate solutions in the tropics. *Philos. Trans. R. Soc. B* **375**, 20190126 (2020).
6. Friedlingstein, P. et al. Global carbon budget 2019. *Earth Syst. Sci. Data* **11**, 1783–1838 (2019).
7. Houghton, R. A. & Nassikas, A. A. Global and regional fluxes of carbon from land use and land cover change 1850–2015. *Glob. Biogeochem. Cycles* **31**, 456–472 (2017).
8. Hansis, E., Davis, S. J. & Pongratz, J. Relevance of methodological choices for accounting of land use change carbon fluxes. *Glob. Biogeochem. Cycles* **29**, 1230–1246 (2015).
9. Pan, Y. et al. A large and persistent carbon sink in the world's forests. *Science* **333**, 988–993 (2011).
10. IPCC. *2006 IPCC Guidelines for National Greenhouse Gas Inventories Vol. 4* (eds Eggleston, S. et al.) (IGES, 2006).
11. IPCC. *2019 Refinement to the 2006 IPCC Guidelines for National Greenhouse Gas Inventories Vol. 4* (eds Buendia, E. C. et al.) (IPCC, 2019).
12. Grassi, G. et al. Reconciling global-model estimates and country reporting of anthropogenic forest CO<sub>2</sub> sinks. *Nat. Clim. Change* **8**, 914–920 (2018).
13. Lee, D., Llopis, P., Waterworth, R., Roberts, G. & Pearson, T. *Approaches to REDD+ Nesting: Lessons Learned from Country Experiences* (World Bank, 2018).
14. Streck, C. et al. *Options for Enhancing REDD+ Collaboration in the Context of Article 6 of the Paris Agreement* (Meridian Institute, 2017).
15. Hansen, M. C. et al. High-resolution global maps of 21st-century forest cover change. *Science* **342**, 850–853 (2013).
16. *World Database on Protected Areas User Manual* (UNEP, 2016); <https://www.protectedplanet.net/en/resources/wdpa-manual>
17. Curtis, P. G., Slay, C. M., Harris, N. L., Tyukavina, A. & Hansen, M. C. Classifying drivers of global forest loss. *Science* **361**, 1108–1111 (2018).
18. Saatchi, S. S. et al. Benchmark map of forest carbon stocks in tropical regions across three continents. *Proc. Natl Acad. Sci. USA* **108**, 9899–9904 (2011).
19. *PRODES Deforestation* (INPE, 2019); <http://www.obt.inpe.br/OBT/assuntos/programas/amazonia/prodes>
20. Ogle, S. M. et al. Delineating managed land for reporting national greenhouse gas emissions and removals to the United Nations framework convention on climate change. *Carbon Balance Manag.* **13**, 9 (2018).
21. Pearson, T. R., Brown, S., Murray, L. & Sidman, G. Greenhouse gas emissions from tropical forest degradation: an underestimated source. *Carbon Balance Manag.* **12**, 3 (2017).
22. Ahlström, A. et al. The dominant role of semi-arid ecosystems in the trend and variability of the land CO<sub>2</sub> sink. *Science* **348**, 895–899 (2015).
23. Van Der Werf, G. R. et al. Global fire emissions estimates during 1997–2016. *Earth Syst. Sci. Data* **9**, 697–720 (2017).
24. Kirschbaum, M. U., Zeng, G., Ximenes, F., Giltrap, D. L. & Zeldis, J. R. Towards a more complete quantification of the global carbon cycle. *Biogeosciences* **16**, 831–846 (2019).
25. Global Forest Observations Initiative. *Integration of Remote-sensing and Ground-based Observations for Estimation of Emissions and Removals of Greenhouse Gases in Forests* 2nd edn (FAO, 2016).
26. Potapov, P. et al. Annual continuous fields of woody vegetation structure in the Lower Mekong region from 2000–2017 Landsat time-series. *Remote Sens. Environ.* **232**, 111278 (2019).
27. Federici, S., Lee, D. & Herold, M. *Forest Mitigation: A Permanent Contribution to the Paris Agreement?* (Climate and Land Use Alliance, 2017).
28. Romijn, E. et al. Assessing change in national forest monitoring capacities of 99 tropical countries. *Ecol. Manag.* **352**, 109–123 (2015).
29. Cook-Patton, S. Mapping potential carbon capture from global natural forest regrowth. *Nature* **585**, 545–550 (2020).
30. *The Global Stocktake* (UNFCCC, 2015); <https://unfccc.int/topics/science/workstreams/global-stocktake-referred-to-in-article-14-of-the-paris-agreement>

**Publisher's note** Springer Nature remains neutral with regard to jurisdictional claims in published maps and institutional affiliations.

© The Author(s), under exclusive licence to Springer Nature Limited 2021

## Methods

**Study design and scope.** We mapped gross and net GHG emissions by sources and removals by sinks from global forest lands by synthesizing information collected from more than 637,000 ground plots, 707,561 waveform lidar observations and other satellite data into a spatial forest carbon monitoring framework. The analysis covers 2001 to 2019 but can be extended to include later years as data are updated. To the extent possible, we adhered to IPCC Guidelines developed for the agriculture, forestry and other land use (AFOLU) sector<sup>10,11</sup>. In the context of IPCC land-use categories, our analysis covers only forest-related transitions (forest to non-forest, non-forest to forest and forest remaining forest). We applied the IPCC gain-loss method (versus the stock-difference method<sup>10</sup>), in which forest carbon (C) stocks in five ecosystem pools were estimated for a base year (2000) after which changes in C stocks were estimated by considering both annual C losses from land-use change and disturbance (conventionally represented by a + sign) as well as annual C gains from forest regrowth (represented by a - sign). We included harvested wood products as a sixth (human-created) carbon pool. We also included methane ( $\text{CH}_4$ ) and nitrous oxide ( $\text{N}_2\text{O}$ ) emissions from stand-replacement forest fires and drainage of organic soils associated with a loss of tree cover. We summarized GHG fluxes across all relevant gases and reported in units of  $\text{CO}_2$  equivalents ( $\text{CO}_2\text{e}$ ) using 100-yr Global Warming Potentials (without climate feedbacks) from the IPCC Fifth Assessment Report<sup>1</sup>.

We set all data inputs to a common resolution of  $0.00025^\circ \times 0.00025^\circ$  to match the resolution of Landsat-based tree cover change data of Hansen et al.<sup>15</sup>. Gross emissions and removals were modelled at this common resolution across approximately 90 billion individual pixels of global forest cover (defined below). We resampled all input layers to this resolution so that outputs can be flexibly aggregated to larger scales. Extended Data Fig. 10 summarizes the overall conceptual approach and Supplementary Table 3 provides a list of data inputs.

**Forest definition and extent.** Initially, we defined forest extent in the year 2000 similarly to Hansen et al.<sup>15</sup>, that is, any 30-m Landsat pixel that met a tree canopy threshold of at least 30% with trees taller than 5 m in height. This initial definition included natural and seminatural forests, plantations and agricultural tree crops such as oil palm and agroforestry systems where minimum height and cover thresholds were met. On the basis of available data, we made four modifications to the original tree cover map to refine our global map of forest extent:

1. We included pixels of tree cover gain since 2000 in addition to tree cover already present in the year 2000.
2. We included only tree cover pixels that also had a corresponding value in the aboveground biomass density map (0.031% of tree cover pixels lacked a biomass value).
3. We excluded all areas of tree cover falling within oil palm plantation boundaries mapped for the year 2000 in Indonesia and Malaysia<sup>31–34</sup>.
4. We replaced tree cover extent from Hansen et al.<sup>15</sup> with mangrove forest extent using data from Giri et al.<sup>35</sup>; in areas of geographic overlap, mangroves had priority.

**Forest aboveground live biomass density in 2000.** We created a year 2000 map of aboveground live biomass density (AGB, in  $\text{Mg ha}^{-1}$ ) at 30-m resolution by combining two maps: one developed specifically for mangroves<sup>36</sup> and the other developed to cover all woody vegetation globally (Supplementary Data 1). In areas of geographic overlap, the mangrove biomass map had priority. The basic approach is the same as that used to map tropical biomass at 500-m (ref. <sup>37</sup>) and 30-m (ref. <sup>38</sup>) resolution; published height-biomass equations were applied to estimate biomass over specific regions and forest types around the world (Extended Data Fig. 1a). These equations, developed by linking observations from airborne or spaceborne lidar to 20,347 ground-measured biomass plots, were applied to estimate aboveground biomass density from spaceborne lidar observations across 707,561 locations globally. To create a continuous biomass map (Extended Data Fig. 1b), separate random forest models were trained for each of six biogeographic realms using predictor variables of Landsat imagery (bands 3, 4, 5 and 7), normalized difference vegetation index (NDVI), normalized difference infrared index (NDII), mean percentage tree cover, mean elevation, mean slope and monthly mean precipitation, temperature and bioclimatic data. Additional details are provided in Supplementary Data 1.

**Forest ecosystem carbon pools in 2000.** From the 30-m global AGB map, we mapped belowground live biomass density (BGB) using a forest root-to-shoot ratio<sup>39</sup> with mangrove-specific ratios based on defaults provided in Table 4.5 of the 2013 IPCC Wetlands Supplement<sup>40</sup>. AGB and BGB values were converted to C density values using a biomass-to-carbon ratio of 0.45 for mangroves<sup>40</sup> and 0.47 for all other forest types<sup>10,11</sup>. From the final 30-m AGB map we estimated dead wood and litter biomass densities per pixel as constant fractions of AGB using a lookup table based on global ecological zone, elevation and precipitation regime<sup>41</sup> (Supplementary Table 4). Dead wood and litter biomass densities were converted to C densities using IPCC conversion factors<sup>10</sup>.

Soil organic carbon density in the top 30 cm of mineral soils was mapped using SoilGrids250 (v.2.0)<sup>42</sup> after resampling from its original spatial resolution of 250 m

to match the common 30-m resolution of our analysis. For mangrove forests, we used a 30-m soil carbon map developed specifically for mangroves<sup>43</sup>. We delineated locations of organic (peat) soils using maps summarized in Supplementary Table 3.

We used these five forest carbon pool maps as the basis for estimating emission factors associated with various forest disturbances (see below).

**Activity data.** Activity data were defined using the global forest change product of Hansen et al.<sup>15</sup> with loss updated annually on Global Forest Watch. In the model, all pixels defined as forest were classified into one of four categories: (1) loss only; (2) gain only; (3) both loss and gain; or (4) no change over the period 2001–2019. Loss is defined by Hansen et al. as a stand-replacement disturbance and includes all disturbances (natural and anthropogenic) observable in Landsat imagery. Gain is defined as a non-forest to forest change, which includes tree cover gain observed after harvest and other disturbance. The loss product is annual, while the gain product represents a cumulative total (2000–2012). Loss and gain can co-occur on pixels undergoing forest management or other forms of disturbance and regrowth. Lack of annually updated gain data is addressed through the sensitivity analysis (Extended Data Fig. 5). Due to a lack of information about tree cover gain after 2012, we assumed no additional areas of gain from 2012 to 2019. Areas of no change reflect forest areas established before 2000 that showed no observable disturbance in Landsat imagery between 2000 and 2019.

**Emission factors.** We assigned emission factors to tree cover loss pixels following an IPCC land-use classification framework, on the basis of whether each pixel maintained its land use or was converted to a new use over the analysis period. Since forest may remain in the same use despite a temporary loss of tree cover, we used the global 10-km map of Curtis et al.<sup>17</sup> (updated through 2019) to attribute tree cover loss to one of five dominant drivers; these influence the C pools affected (Supplementary Table 5) and thus the emission factors assigned to each individual loss pixel. Supplementary Table 6 summarizes emission factors by forest type within each climate domain.

**Commodity-driven deforestation and shifting agriculture.** The initial change in C stocks was estimated as a full loss of C in aboveground, belowground, dead wood and litter pools. In addition to  $\text{CO}_2$  emissions resulting from a loss of C stocks, we used IPCC equation 2.27 (ref. <sup>10</sup>) and a 1-km global burned area map<sup>44</sup> to calculate  $\text{CH}_4$  and  $\text{N}_2\text{O}$  emissions in loss pixels that overlapped with areas that burned the same year or the year before (to account for lag effects between fire occurrence and observed tree cover loss). For deforestation on mineral soils, soil C loss was estimated using IPCC equation 2.25 (ref. <sup>10</sup>); default soil stock change factors vary by ecological zone and were assigned spatially using ecozone boundaries<sup>45</sup>. Per IPCC guidelines, 1/20th of the total soil C stock change was apportioned annually from the year of loss through the last year of the analysis period (2019) but assigned to the year of observed tree cover loss. Due to lack of information in the driver attribution map<sup>17</sup> about the specific land use established after forest clearing, we assumed for the purposes of soil emission accounting that all deforested land on mineral soils for commodity-driven deforestation was converted to annual cropland with full tillage and medium inputs. A different factor was used to estimate loss of soil C on mineral soils (Table 5.10 in the IPCC Guidelines<sup>10</sup>) in areas of shifting agriculture, which were assumed to represent transient land-use conversions to cropland under shortened fallow, where vegetation recovery is not attained before re-clearing. Soil emissions were not estimated for areas of loss on mineral soils that overlapped with forest and wood fibre plantations, even if they fell within the broader commodity-driven deforestation or shifting agriculture classes, consistent with the assumption that loss of tree cover within tree plantations follows the forestry assumptions listed in Supplementary Table 5 (see emissions from Forestry below). For loss on organic soils that overlapped with tropical plantations and tree crops planted since 2000, GHG emissions associated with drainage were estimated using  $\text{CO}_2$  and  $\text{CH}_4$  emission factors provided in the IPCC Wetlands Supplement<sup>40</sup>. Like emissions from mineral soils, emissions from peat drainage were assumed to continue in each year after loss up through the last year of the analysis period (2019) but were assigned to the year of observed tree cover loss. Emissions ( $\text{CO}_2$ ,  $\text{CH}_4$  and  $\text{N}_2\text{O}$ ) from peat burning were also calculated on the basis of methods provided in the IPCC Wetlands Supplement<sup>40</sup> where a loss pixel overlapped with areas burned the same year, or the year before, the loss event (on the basis of global burned area data).

**Urbanization.** The same assumptions and calculations were used for calculating gross emissions from urbanization as for commodity-driven deforestation and shifting agriculture, except a different factor was used to estimate the loss of soil C on mineral soils. We assumed that forest land converted to settlement was paved over and applied the IPCC default assumption<sup>11</sup> that 20% of the soil C relative to the previous land use was lost as a result of disturbance, removal or relocation.

**Forestry.** Emission factors for loss attributed to forestry were estimated as the loss of C in live biomass only, following assumptions outlined in Supplementary Table 5 that there is no net change to the dead organic matter or soil C pools in the case of mineral soils. Emissions from peat drainage and burning associated with forestry activities, as well as non- $\text{CO}_2$  emissions in the case of forest fires, were included in

the same way as for deforestation and shifting agriculture above. Emission factors for loss pixels within the ‘zero or minor loss’ category of the driver attribution map also followed assumptions for forestry (Supplementary Table 5).

**Wildfire.** Within 10-km grid cells of the drivers map labelled wildfire, wildfire emission factors were applied only for 30-m pixels where loss occurred in the year of, or year after, a fire event in the 1-km burned area map. In these cases, we used IPCC equation 2.27 (ref. <sup>10</sup>) to estimate both CO<sub>2</sub> and non-CO<sub>2</sub> emissions from forest fire. The AGB map determined the mass of fuel available for combustion and a lookup table (Table 2.6 of the IPCC Guidelines<sup>10</sup>) provided default combustion and emission factors that were applied on the basis of forest type (primary versus secondary). For boreal and temperate forests, combustion factors were applied on the basis of the assumption of a land-clearing fire, given that forest loss is defined in Hansen et al.<sup>15</sup> as a stand-replacement disturbance. In cases where organic soils overlapped with burned areas, emissions from peat burning (CO<sub>2</sub>, CH<sub>4</sub> and N<sub>2</sub>O) were estimated following guidance in the IPCC Wetlands Supplement<sup>40</sup>. Forestry emission factors, rather than wildfire factors, were applied where loss did not overlap with a fire event in the 1-km burned area map.

**Removal factors.** We developed removal factors spatially by linking information about each pixel’s geographic region, ecological zone, forest type and age class to corresponding growth rates on the basis of best available information. Supplementary Table 6 summarizes removal factors by forest type in each climate domain. In areas of geographic overlap, the priority of assigning removal factors to a given pixel reflects the order of data sources listed below. Removal factors include accumulation in live biomass only and reflect the net increase, accounting for both productivity and mortality. We assumed no change to the dead organic matter and soil organic carbon pools, consistent with the IPCC Tier 1 assumption of no net change to non-biomass pools in forest land remaining forest land. The number of years of carbon accumulation was assigned as 19 yr for undisturbed forest, 6 yr for areas of new tree cover gain and one less than the year in which tree cover loss occurred for loss-only forest.

**Mangroves.** We applied mangrove-specific growth rates and root-to-shoot ratios from IPCC Tables 4.4 and 4.5 of the Wetlands Supplement<sup>40</sup>, respectively.

**Europe.** We assigned removal factors spatially according to a map of dominant tree species developed from 260,000 national inventory plot locations<sup>46</sup>. For each species, we estimated mean annual increment (MAI) values from Table 4.11 of the updated IPCC Guidelines<sup>11</sup>, FAO Planted Forest Assessment<sup>47</sup> and national inventories<sup>48</sup> (Supplementary Table 3). These were converted to aboveground biomass growth rates using species-specific biomass conversion and expansion factors and belowground biomass increment was added on the basis of a root-to-shoot ratio<sup>39</sup>.

**Plantations and tree crops.** Outside Europe, we assigned removal factors for plantations and tree crops using a variety of published data sources<sup>49</sup>. For common plantation species, we used MAI and biomass conversion and expansion factors summarized in the updated IPCC Guidelines<sup>11</sup> to estimate aboveground biomass increment and added belowground biomass increment on the basis of a root-to-shoot ratio<sup>39</sup>. Rates in plantations were assigned on the basis of mapped species when known or, when unknown, the most common mix of plantation species grown in the region. Removal factors for tree crops such as oil palm and rubber as well as various types of agroforestry systems were estimated for areas mapped as such on the basis of regionally specific values derived from the published literature and from Tables 5.1 and 5.3 of the updated IPCC Guidelines<sup>11</sup>. All removal factors used for plantations and tree crops, along with data sources and assumptions applied, are provided in the companion spatial attribute file associated with the global compilation of planted tree maps used in this analysis<sup>49</sup>.

**United States.** We developed removal factors for three age classes (0–20, 20–100 and >100 yr) for forest types across 11 geographic regions using methods broadly similar to those of Smith et al.<sup>50</sup>, except that we included more forest types in each region, as well as more recent and comprehensive data from the US Forest Inventory and Analysis database. Removal factors were developed from approximately 130,000 inventory plot locations. Pixels were assigned removal factors on the basis of dominant forest type<sup>51</sup>, age class<sup>52</sup> and geographic inventory region.

**Young secondary forests.** Outside the United States and Europe, areas of tree cover gain that fell outside boundaries of mangroves<sup>35</sup> and planted trees<sup>49</sup> were assumed to be secondary natural forest regrowth <20 years old. We assigned natural forest regrowth removal factors to these areas using the 1-km map of Cook-Patton et al.<sup>29</sup>.

**Primary forests.** We used removal factors by ecological zone and continent from IPCC Table 4.9 of the 2019 IPCC Refinement<sup>11</sup> and assigned them spatially between 30°N and 30°S within a tropical primary humid forest map<sup>53</sup>. Outside 30°N and 30°S, we used a map of intact forest landscapes<sup>54</sup> as a proxy for primary forests, which is likely to be highly conservative due to the relatively large extent

criterion applied but represents the best available information by which to spatially delineate primary from old secondary forests in boreal and temperate regions.

**Old secondary forests.** We assigned removal factors from IPCC Table 4.9 (>20 yr) to all forest areas that fell outside the types identified above. Given no observed disturbance occurred in these areas since the year 2000, we assumed they were secondary natural forests at least 20 years old.

**Harvested wood products.** We used statistics reported in FAOSTAT and methods outlined in the 2019 Refinement<sup>11</sup> to estimate emissions and/or removals arising from harvested wood products. Losses of harvested wood products in use were assumed to result in CO<sub>2</sub> emissions to the atmosphere, with no explicit representation of the subsequent retention of disposed wood in solid waste disposal sites (SWDS) and eventual CO<sub>2</sub> emissions from SWDS. Calculations rely on statistics reported by countries on production, import and export volumes for three aggregate semifinished wood product commodity classes: sawnwood, wood-based panels and paper and paperboard.

**Uncertainty analysis.** We estimated uncertainty in GHG flux estimates globally and at the scale of climate domains by combining uncertainties in the activity data and emission/removal factors following a Taylor series statistical approach as in Roman-Cuesta et al.<sup>55</sup> and Carter et al.<sup>56</sup>. This approach underlies the IPCC Approach 1 (simple error propagation)<sup>10</sup> and produces similar results but reflect exact calculations of variances and s.d., whereas IPCC Approach 1 is an approximated approach that yields 95% confidence intervals.

Uncertainties of all major components of the flux model were included (activity data, affected C pools of the emission/removal factors, combustion and emission factor uncertainties for fire-related emissions). Errors were assumed to be statistically independent (uncorrelated), normally distributed and without bias. Supplementary Table 1 shows the contribution of each uncertainty component for domain and global gross emissions, removals and net flux, reported as the percentage reduction in output variances as each of the uncertainty components were assumed to have no variance. Variance of the net GHG flux was reduced the most when removing variance of the removal factor for temperate forests older than 20 yr. Variances are likely to be lower when estimated across smaller geographic regions. Estimation of uncertainty is currently limited to the global and biome scales based on available data for estimating uncertainty in the activity data.

**Reporting Summary.** Further information on research design is available in the Nature Research Reporting Summary linked to this article.

## Data availability

Geospatial data generated from the current study are publicly available on Global Forest Watch’s Open Data Portal (<http://data.globalforestwatch.org/>) and from the corresponding author upon request. Summary geospatial statistics are available from the corresponding author upon request. All data inputs used in the current study are publicly available or were obtained by the corresponding author.

## Code availability

To ensure full reproducibility and transparency of our research, we provide all of the scripts used in our analysis. Codes used for this study are permanently and publicly available on GitHub (<https://github.com/wri/carbon-budget>).

## References

31. Austin, K. et al. Shifting patterns of oil palm driven deforestation in Indonesia and implications for zero-deforestation commitments. *Land Use Policy* **69**, 41–48 (2017).
32. Gaveau, D. L. et al. Four decades of forest persistence, clearance and logging on Borneo. *PLoS ONE* **9**, e101654 (2014).
33. Miettinen, J., Shi, C. & Liew, S. C. Land cover distribution in the peatlands of Peninsular Malaysia, Sumatra and Borneo in 2015 with changes since 1990. *Glob. Ecol. Conserv.* **6**, 67–78 (2016).
34. Gunarso, P., Hartoyo, M., Agus, F. & Killeen, T. in *Reports from the Technical Panels of the 2nd Greenhouse Gas Working Group of the Roundtable on Sustainable Palm Oil* (eds Killeen, T. J. & Goon, J.) 29–64 (RSPO, 2013).
35. Giri, C. et al. Status and distribution of mangrove forests of the world using earth observation satellite data. *Glob. Ecol. Biogeogr.* **20**, 154–159 (2011).
36. Simard, M. et al. Mangrove canopy height globally related to precipitation, temperature and cyclone frequency. *Nat. Geosci.* **12**, 40–45 (2019).
37. Baccini, A. et al. Estimated carbon dioxide emissions from tropical deforestation improved by carbon-density maps. *Nat. Clim. Change* **2**, 182–185 (2012).
38. Zarin, D. J. et al. Can carbon emissions from tropical deforestation drop by 50% in 5 years? *Glob. Change Biol.* **22**, 1336–1347 (2016).
39. Mokany, K., Raison, R. J. & Prokushkin, A. S. Critical analysis of root: shoot ratios in terrestrial biomes. *Glob. Change Biol.* **12**, 84–96 (2006).

40. IPCC *Supplement to the 2006 IPCC Guidelines for National Greenhouse Gas Inventories: Wetlands* (eds Hiraishi, T. et al.) (IPCC, 2014).
41. *Methodological Tool: Estimation of Carbon Stocks and Change in Carbon Stocks in Dead Wood and Litter in A/R CDM Project Activities* (UNFCCC, 2013); <https://cdm.unfccc.int/methodologies/ARmethodologies/tools/ar-am-tool-12-v3.0.pdf>
42. Hengl, T. et al. SoilGrids250m: global gridded soil information based on machine learning. *PLoS ONE* **12**, e0169748 (2017).
43. Sanderman, J. et al. A global map of mangrove forest soil carbon at 30 m spatial resolution. *Environ. Res. Lett.* **13**, 055002 (2018).
44. Giglio, L., Boschetti, L., Roy, D. P., Humber, M. L. & Justice, C. O. The Collection 6 MODIS burned area mapping algorithm and product. *Remote Sens. Environ.* **217**, 72–85 (2018).
45. *Global Ecological Zones for FAO Forest Reporting: 2010 Update* (FAO, 2012).
46. Brus, D. et al. Statistical mapping of tree species over Europe. *Eur. J. Res.* **131**, 145–157 (2012).
47. Del Lungo, A., Ball, J. & Carle, J. *Global Planted Forests Thematic Study: Results and Analysis* (FAO, 2006); <http://www.fao.org/forestry/12139-03441d093f070ea7d7c4e3ec3f306507.pdf>
48. *Portugal National Greenhouse Gas Inventory submitted to the UNFCCC, 1990–2018* (UNFCCC, 2020).
49. Harris, N. L., Goldman, E. D. & Gibbes, S. *Spatial Database on Planted Trees Version 1.0* <https://www.wri.org/publication/spatialdatabase-planted-trees> (WRI, 2019).
50. Smith, J. E., Heath, L. S., Skog, K. E. & Birdsey, R. A. *Methods for Calculating Forest Ecosystem and Harvested Carbon with Standard Estimates for Forest Types of the United States General Technical Report* (USDA, Forest Service, 2006); <https://doi.org/10.2737/NE-GTR-343>
51. Ruefenacht, B. et al. Conterminous US and Alaska forest type mapping using forest inventory and analysis data. *Photogramm. Eng. Remote Sensing* **74**, 1379–1388 (2008).
52. Pan, Y. et al. Age structure and disturbance legacy of North American forests. *Biogeosciences* **8**, 715–732 (2011).
53. Turubanova, S., Potapov, P. V., Tyukavina, A. & Hansen, M. C. Ongoing primary forest loss in Brazil, Democratic Republic of the Congo, and Indonesia. *Environ. Res. Lett.* **13**, 074028 (2018).
54. Potapov, P. et al. The last frontiers of wilderness: tracking loss of intact forest landscapes from 2000 to 2013. *Sci. Adv.* **3**, e1600821 (2017).
55. Roman-Cuesta, R. M. et al. Hotspots of gross emissions from the land use sector: patterns, uncertainties, and leading emission sources for the period 2000–2005 in the tropics. *Biogeosciences* **13**, 4253–4269 (2016).
56. Carter, S. et al. Agriculture-driven deforestation in the tropics from 1990–2015: emissions, trends and uncertainties. *Environ. Res. Lett.* **13**, 014002 (2017).

## Acknowledgements

We thank S. Gibbes for her work on preliminary model development and T. Maschler for his contributions to workflows enabling efficient data processing and generation of summary statistics. Support for this research was funded in part by the Norwegian Ministry of Foreign Affairs (18/2721 Global Forest Watch Achieving Sustainability and Scaling Impact), the UK Department for International Development (DFID FGMC grant no. FGMC2018-21-WRI) and the US Agency for International Development (cooperative agreement no. 7200AA19CA00027 Global Forest Watch 3.0) in support of the Global Forest Watch Partnership convened by the World Resources Institute, by National Aeronautics and Space Administration Earth Science Division NNH12ZDA001 NICESAT2 studies with ICESAT and CryoSat-2 grant no. 12-ICESAT212-0022 to the Woods Hole Research Center and by the NASA Carbon Monitoring System Program Project ‘Estimating Total Ecosystem Carbon in Blue Carbon and Tropical Peatland Ecosystems’ (16- 30 CMS16-0073) to NASA Goddard. The contribution of M.H., S.deB. and D.R.S. was supported by CIFOR’s global comparative study on REDD+ (funded by NORAD), the European Space Agency CCI-Biomass project and the European Commission Horizon 2020 projects VERIFY (grant no. 776810) and REDD-Copernicus (grant no. 821880). Data used in part of this publication were made possible, in part, by an agreement from the United States Department of Agriculture’s Forest Service. This publication may not necessarily express the views or opinions of the Forest Service.

## Author contributions

N.L.H. was involved in conceptualization, data curation, formal analysis, funding acquisition, investigation, methodology, project administration, visualization and writing. D.A.G. contributed to data curation, formal analysis, investigation, methodology, software, validation, visualization and writing. A.B., R.A.B., R.R.C., M.F., L.F., M.C.H., R.A.H., P.V.P., C.M.S., D.R.S., S.S.S. and S.A.T. contributed to data curation, formal analysis, methodology and writing. M.H. contributed to data curation, visualization and writing. S.deB. and A.T. contributed to formal analysis and methodology.

## Competing interests

The authors declare no competing interests.

## Additional information

**Extended data** is available for this paper at <https://doi.org/10.1038/s41558-020-00976-6>.

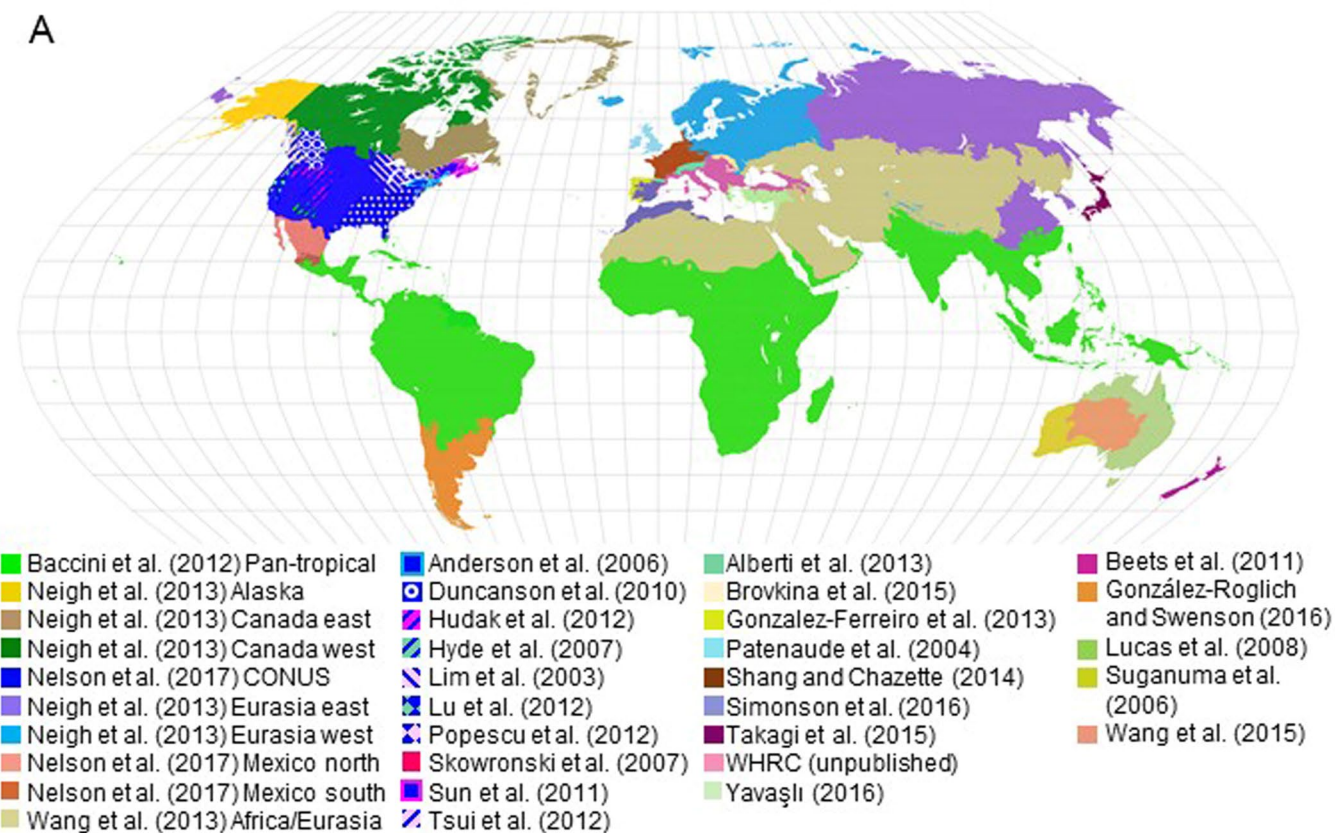
**Supplementary information** is available for this paper at <https://doi.org/10.1038/s41558-020-00976-6>.

**Correspondence and requests for materials** should be addressed to N.L.H.

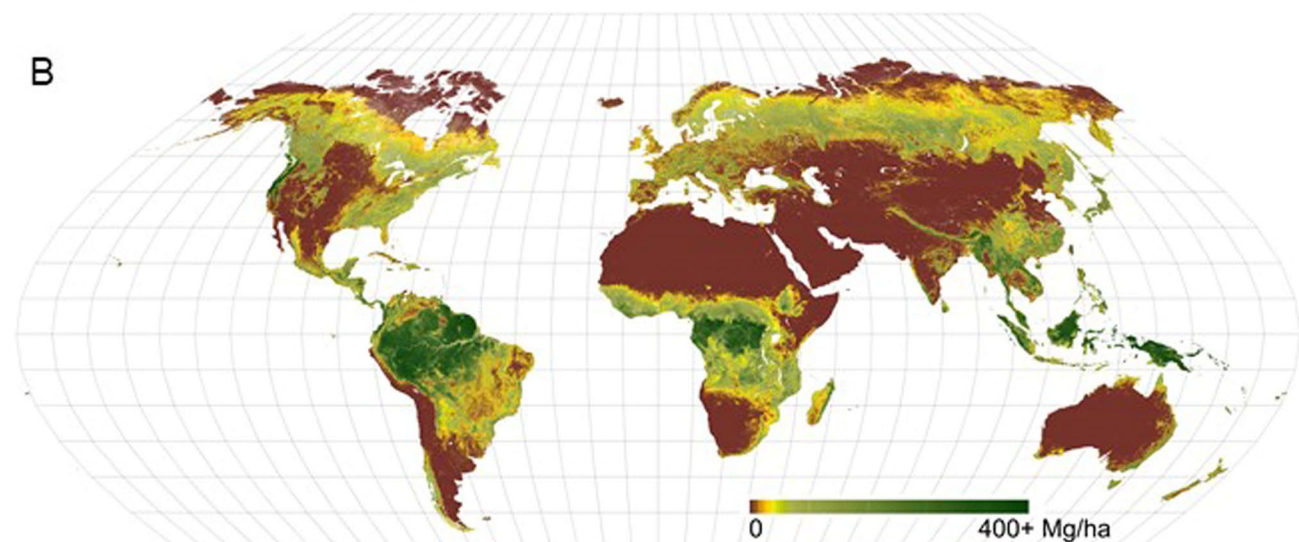
**Peer review information** *Nature Climate Change* thanks Gert-Jan Nabuurs, Seth Spawn and the other, anonymous, reviewer(s) for their contribution to the peer review of this work.

**Reprints and permissions information** is available at [www.nature.com/reprints](http://www.nature.com/reprints).

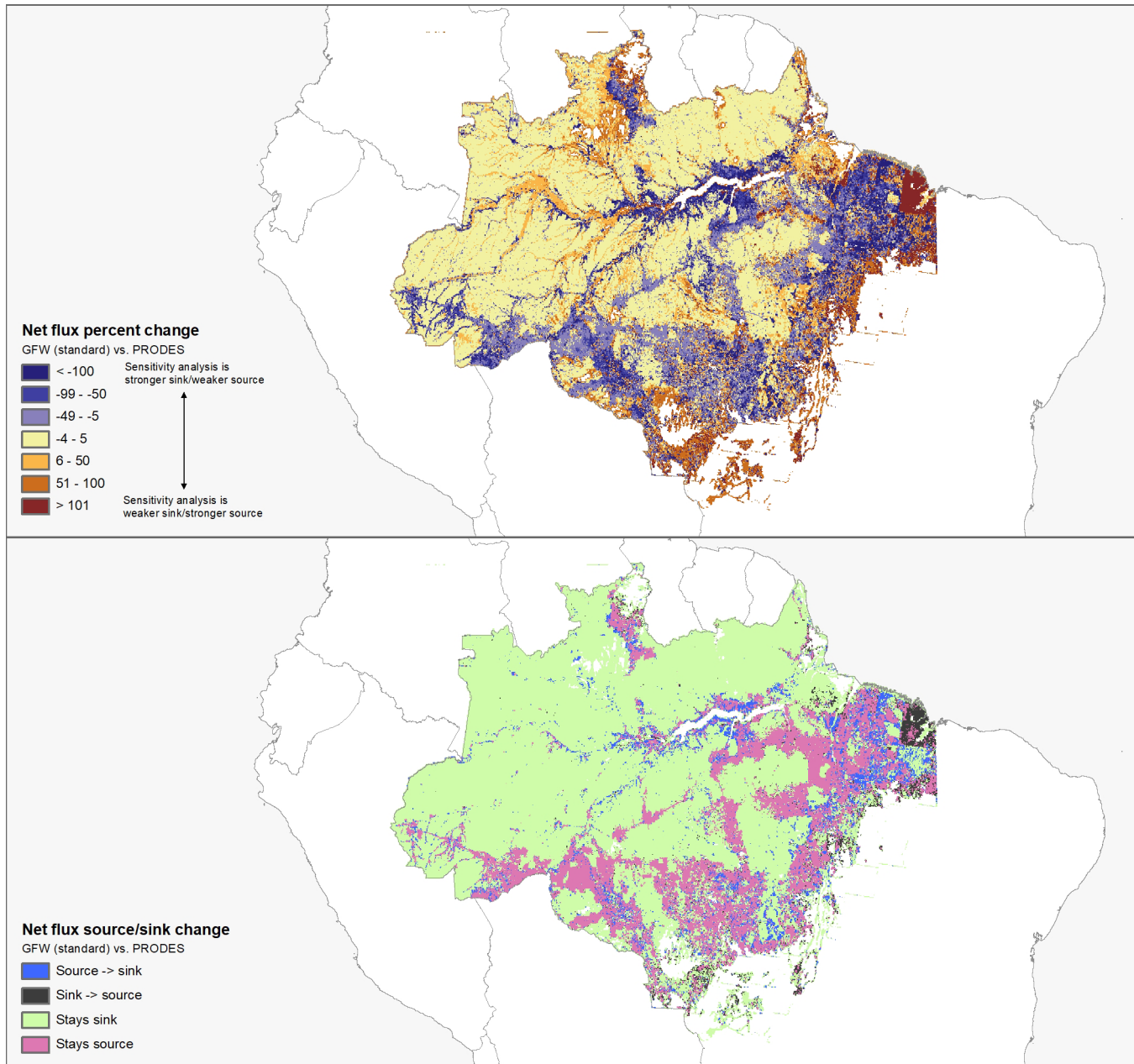
A



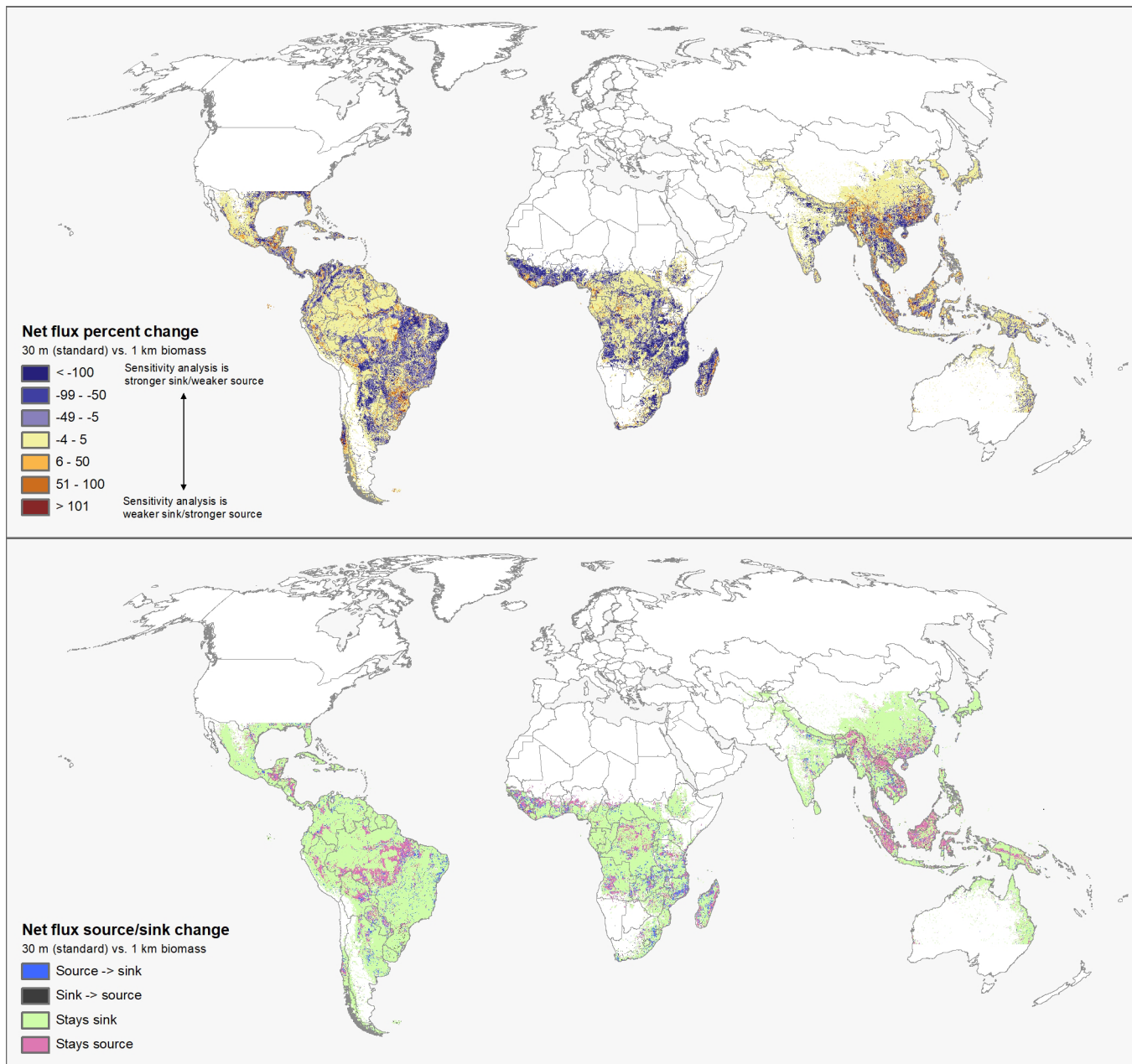
B



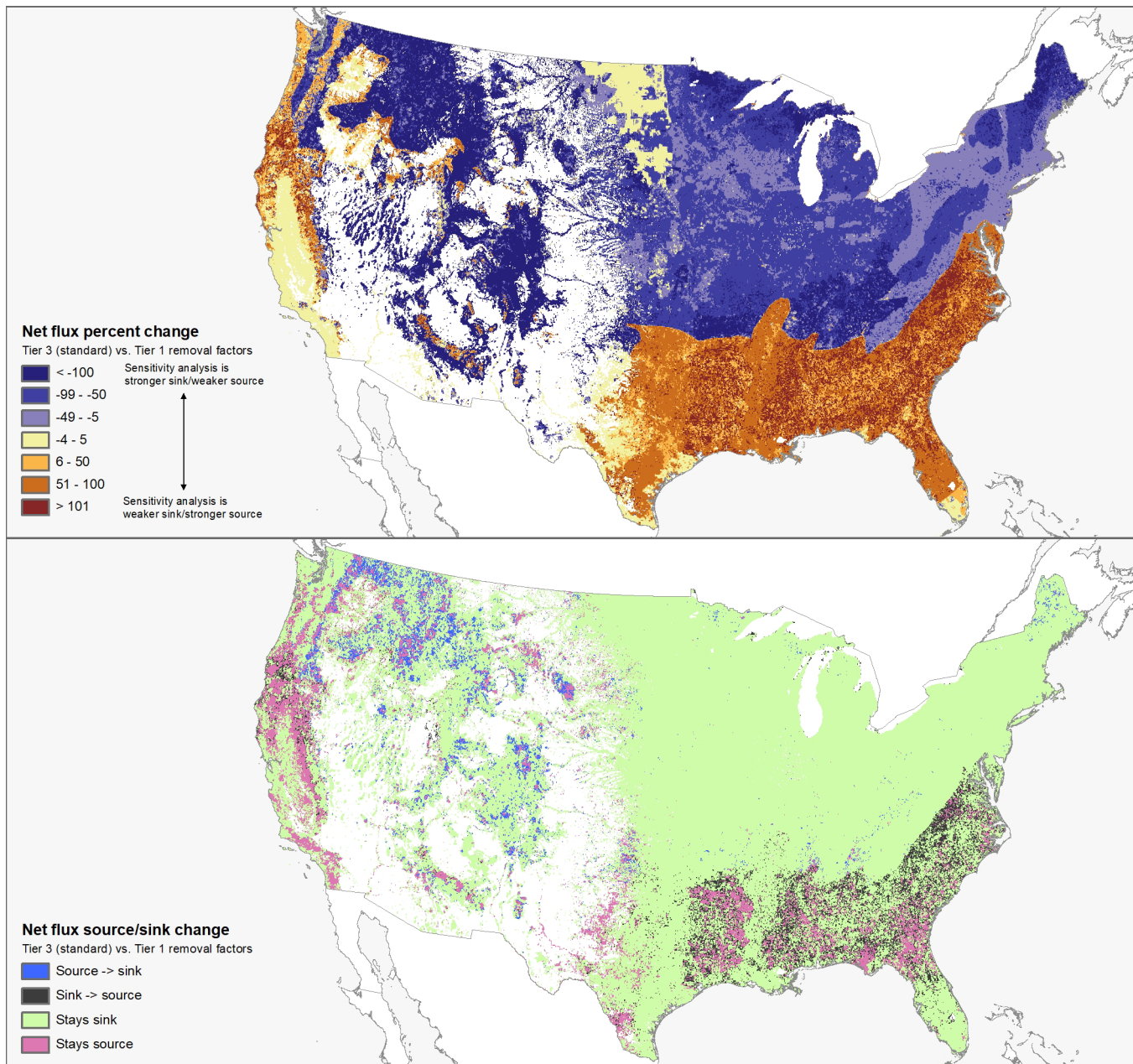
**Extended Data Fig. 1 | Aboveground live woody biomass density in the year 2000.** **a**, Subsets of ecoregions over which different height-biomass equations were applied. Patterned shading indicates equations that were only applied to conifer GLAS shots within the specified ecoregion. **b**, Global 30-m map of aboveground live woody biomass density in the year 2000.



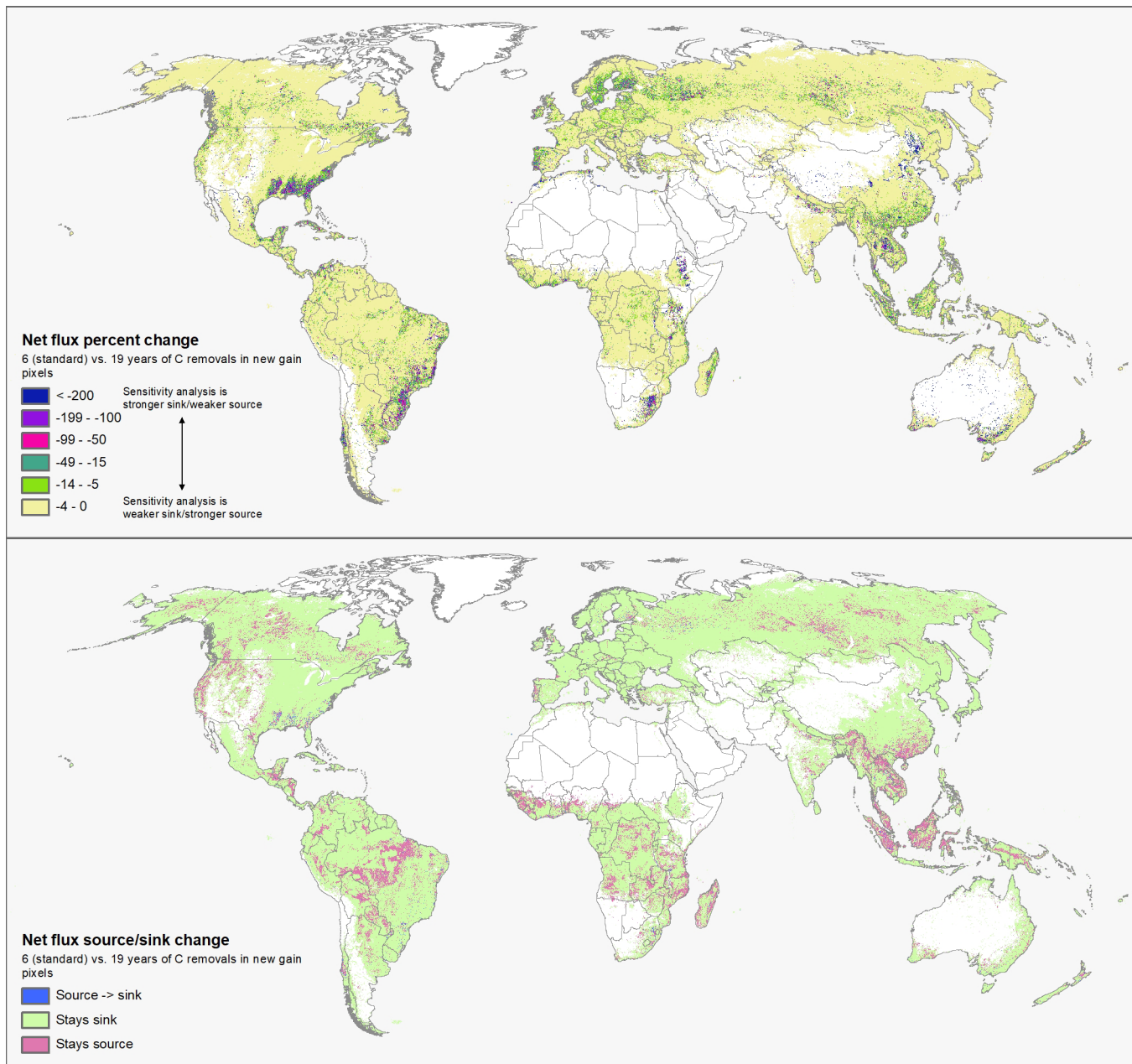
**Extended Data Fig. 2 | Results of sensitivity analysis when the source of tree cover loss data used in the forest GHG flux model is changed from the 30-m tree cover loss product of Hansen et al.<sup>15</sup> in the standard model to PRODES, Brazil's 250-m forest loss monitoring product for the Brazilian Amazon<sup>19</sup>, in the alternative model.** Top panel: Percent change in net GHG flux between standard model and sensitivity analysis model; Bottom panel: Delineation of areas that remain a net GHG source or sink in the sensitivity analysis model vs. those that switch from being a net source or sink to a net sink or source as a result of the changes applied. For display purposes, maps have been resampled from the 30-m observation scale to a 0.04-degree geographic grid.



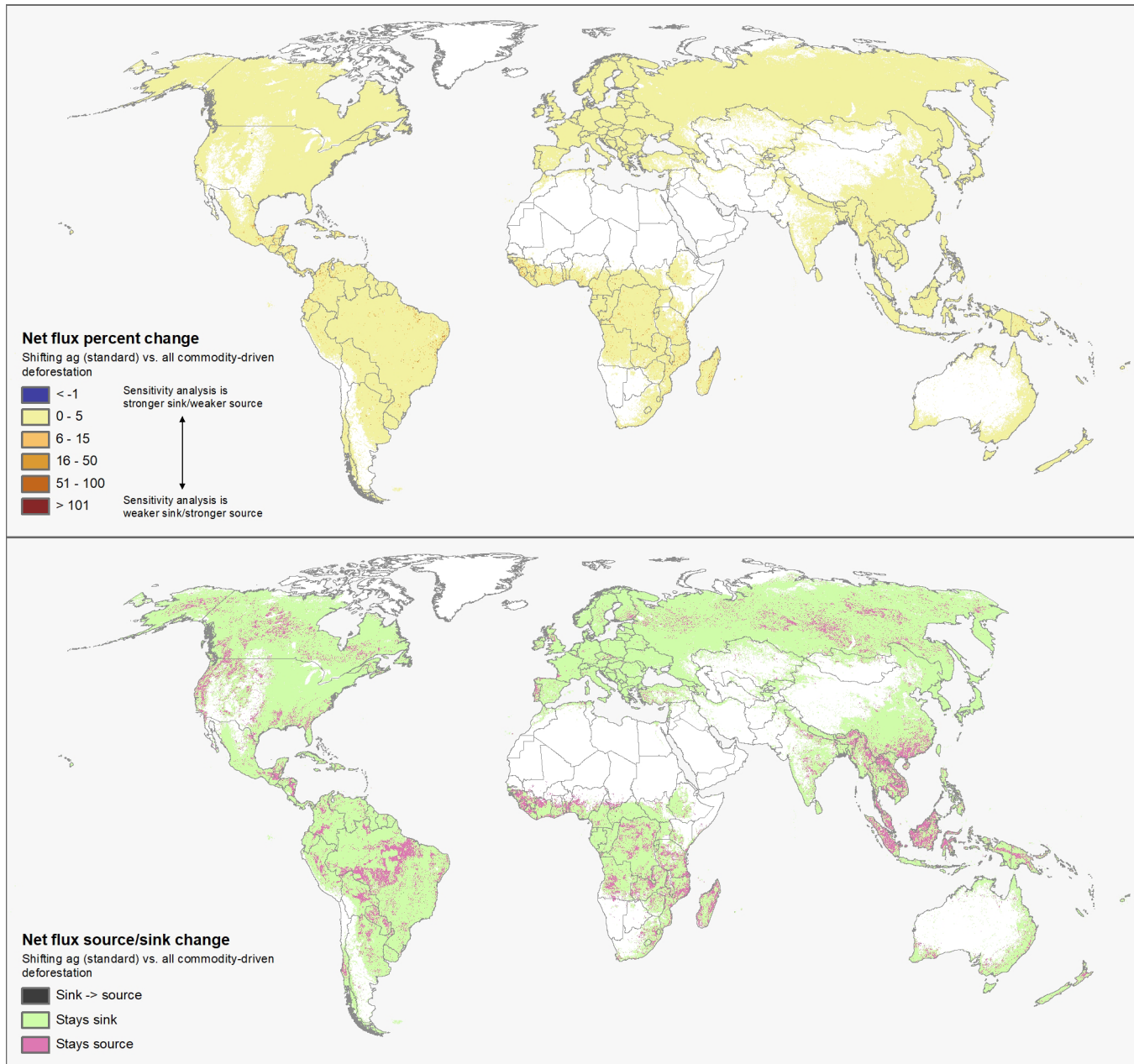
**Extended Data Fig. 3 | Results of sensitivity analysis when the source of biomass data used in the forest GHG flux model is changed from a 30-m global AGB map in the standard model to a 1-km tropical AGB map in the alternative model.** Top panel: Percent change in net GHG flux between standard model and sensitivity analysis model; Bottom panel: Delineation of areas that remain a net GHG source or sink in the sensitivity analysis model vs. those that switch from being a net source or sink to a net sink or source as a result of the changes applied. For display purposes, maps have been resampled from the 30-m observation scale to a 0.04-degree geographic grid.



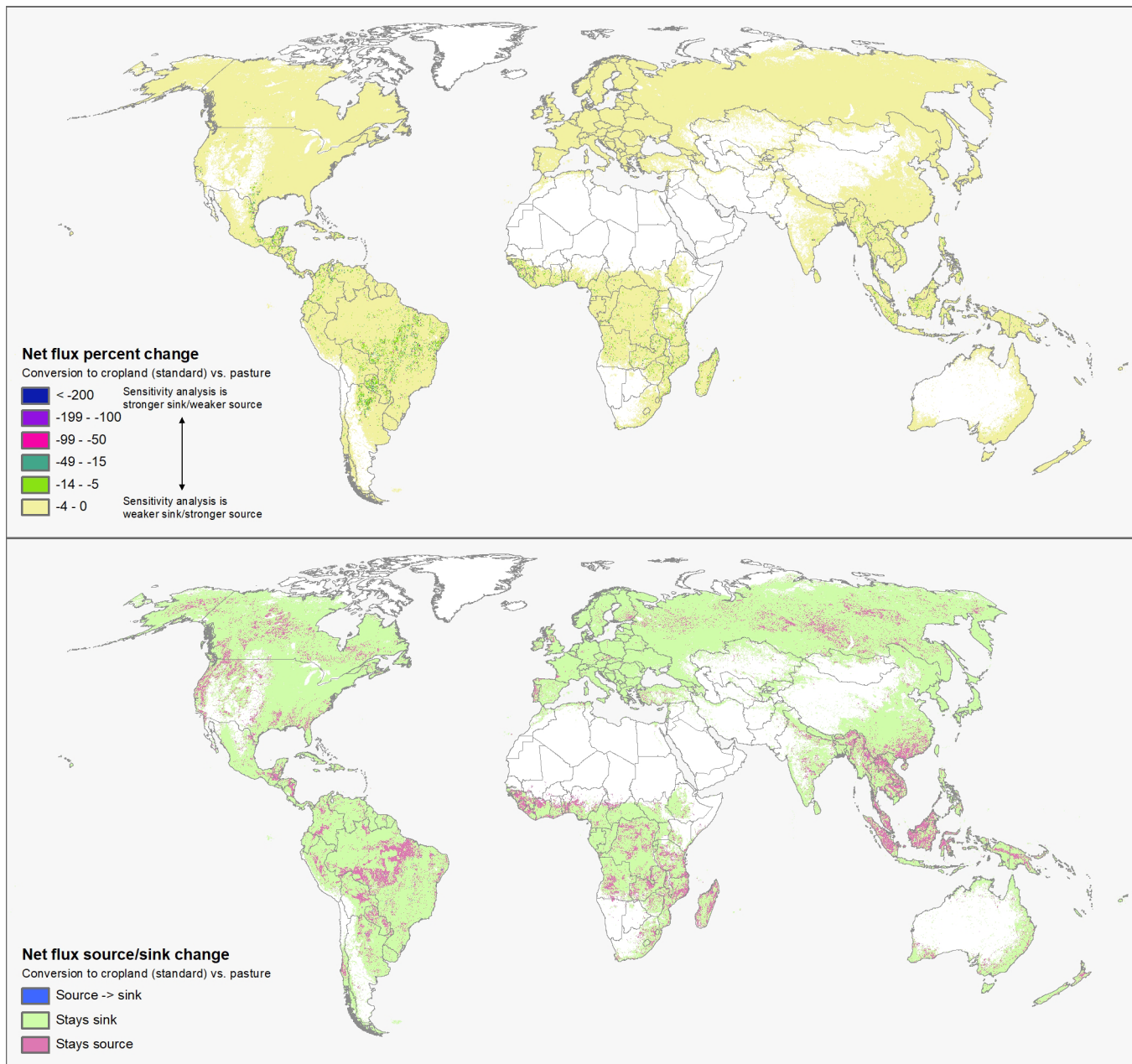
**Extended Data Fig. 4 | Results of sensitivity analysis when rates of AGB accumulation derived from inventory data for different forest types of the United States in the standard model are replaced by IPCC Tier 1 default rates in the alternative model.** Top panel: change in net GHG flux between standard model and sensitivity analysis model; Bottom panel: Delineation of areas that remain a net GHG source or sink in the sensitivity analysis model vs. those that switch from being a net source or sink to a net sink or source as a result of the changes applied. For display purposes, maps have been resampled from the 30-m observation scale to a 0.04-degree geographic grid.



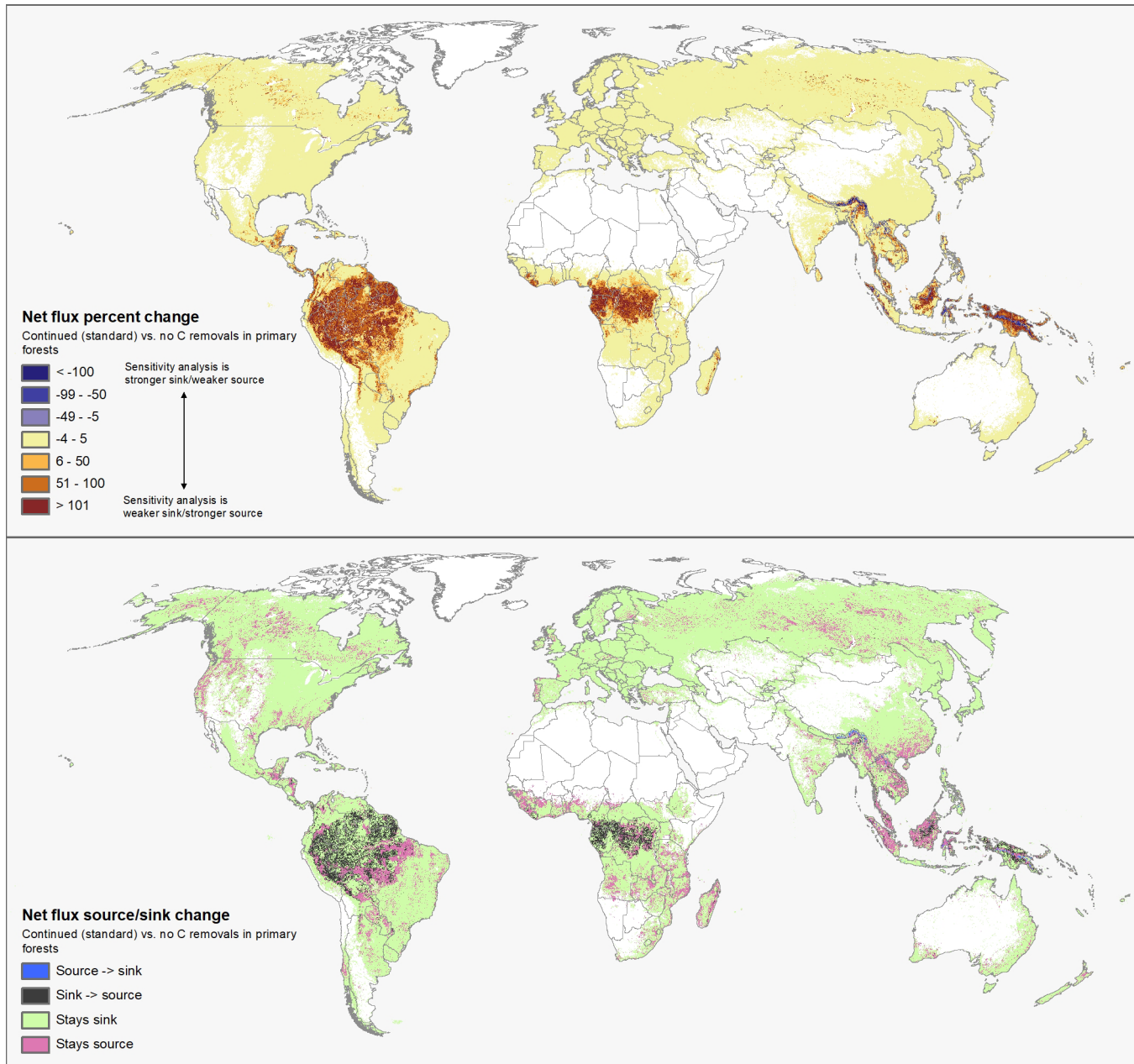
**Extended Data Fig. 5 | Results of sensitivity analysis when the number of years of growth in the GHG flux model is assumed to be 19 in the alternative model vs. 6 in the standard model for pixels of tree cover gain since the year 2000.** Top panel: Percent change in net GHG flux between standard model and sensitivity analysis model; Bottom panel: Delineation of areas that remain a net GHG source or sink in the sensitivity analysis model vs. those that switch from being a net source or sink to a net sink or source as a result of the changes applied. For display purposes, maps have been resampled from the 30-m observation scale to a 0.04-degree geographic grid.



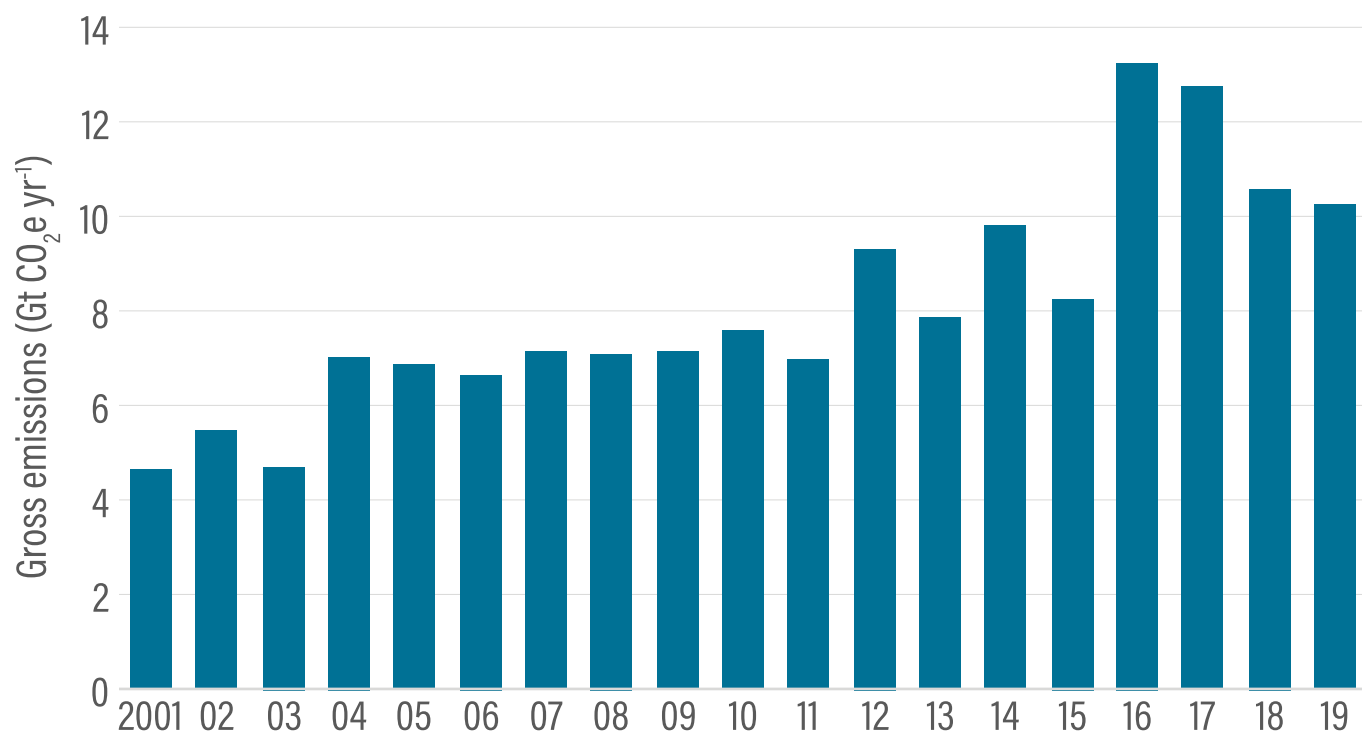
**Extended Data Fig. 6 | Results of sensitivity analysis when tree cover loss in the GHG flux model is attributed to commodity-driven deforestation in the alternative model vs. shifting agriculture in the standard model.** Top panel: Percent change in net GHG flux between standard model and sensitivity analysis model; Bottom panel: Delineation of areas that remain a net GHG source or sink in the sensitivity analysis model vs. those that switch from being a net source or sink to a net sink or source as a result of the changes applied. For display purposes, maps have been resampled from the 30-m observation scale to a 0.04-degree geographic grid.



**Extended Data Fig. 7 | Results of sensitivity analysis when the post- deforestation land-use assumption in the GHG flux model is changed from cropland in the standard model to grassland in the alternative model.** Top panel: Percent change in net GHG flux between standard model and sensitivity analysis model; Bottom panel: Delineation of areas that remain a net GHG source or sink in the sensitivity analysis model vs. those that switch from being a net source or sink to a net sink or source as a result of the changes applied. For display purposes, maps have been resampled from the 30-m observation scale to a 0.04-degree geographic grid.

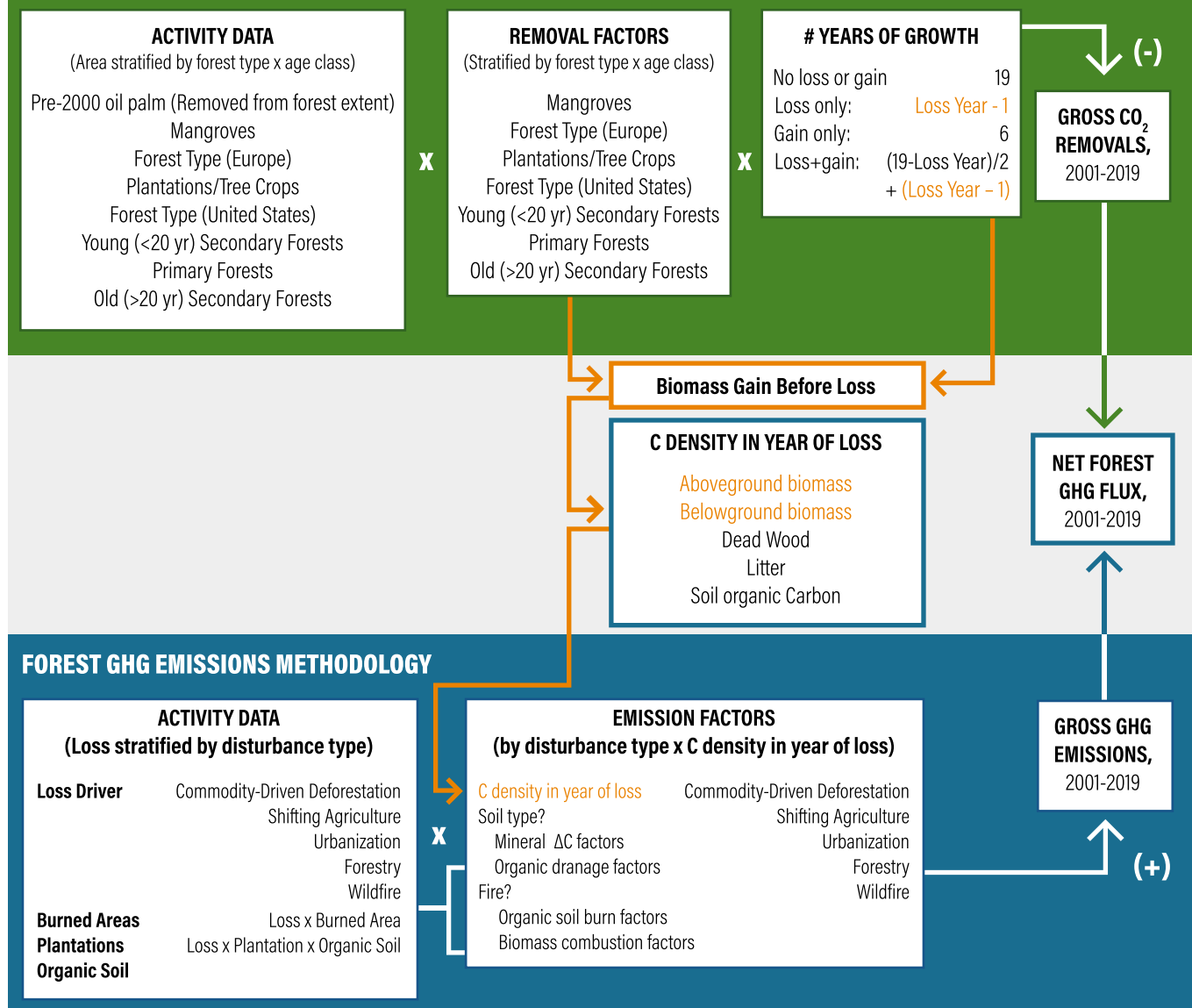


**Extended Data Fig. 8 | Results of sensitivity analysis when assumptions about carbon uptake in primary forests and intact forest landscapes are changed to zero carbon uptake in the alternative model vs. positive carbon uptake in the standard model.** Top panel: Percent change in net GHG flux between standard model and sensitivity analysis model; Bottom panel: Delineation of areas that remain a net GHG source or sink in the sensitivity analysis model vs. those that switch from being a net source or sink to a net sink or source as a result of the changes applied. For display purposes, maps have been resampled from the 30-m observation scale to a 0.04-degree geographic grid.



**Extended Data Fig. 9 | Gross forest-related emissions, 2001–2019.** Emissions reflect all stand-replacement disturbances (natural and anthropogenic) observable in Landsat imagery.

## FOREST CO<sub>2</sub> REMOVALS METHODOLOGY



**Extended Data Fig. 10 | Conceptual framework for modelling forest- related GHG fluxes.** For each 30-m pixel included in the model, gross forest-related emissions and removals are estimated as the product of activity data and emission/removal factors. Net forest GHG flux is the sum of gross fluxes. Text and arrows in orange are portions of the removals methodology that are passed into the emissions methodology.

## Reporting Summary

Nature Research wishes to improve the reproducibility of the work that we publish. This form provides structure for consistency and transparency in reporting. For further information on Nature Research policies, see our [Editorial Policies](#) and the [Editorial Policy Checklist](#).

### Statistics

For all statistical analyses, confirm that the following items are present in the figure legend, table legend, main text, or Methods section.

n/a Confirmed

- The exact sample size ( $n$ ) for each experimental group/condition, given as a discrete number and unit of measurement
- A statement on whether measurements were taken from distinct samples or whether the same sample was measured repeatedly
- The statistical test(s) used AND whether they are one- or two-sided  
*Only common tests should be described solely by name; describe more complex techniques in the Methods section.*
- A description of all covariates tested
- A description of any assumptions or corrections, such as tests of normality and adjustment for multiple comparisons
- A full description of the statistical parameters including central tendency (e.g. means) or other basic estimates (e.g. regression coefficient) AND variation (e.g. standard deviation) or associated estimates of uncertainty (e.g. confidence intervals)
- For null hypothesis testing, the test statistic (e.g.  $F$ ,  $t$ ,  $r$ ) with confidence intervals, effect sizes, degrees of freedom and  $P$  value noted  
*Give P values as exact values whenever suitable.*
- For Bayesian analysis, information on the choice of priors and Markov chain Monte Carlo settings
- For hierarchical and complex designs, identification of the appropriate level for tests and full reporting of outcomes
- Estimates of effect sizes (e.g. Cohen's  $d$ , Pearson's  $r$ ), indicating how they were calculated

*Our web collection on [statistics for biologists](#) contains articles on many of the points above.*

### Software and code

Policy information about [availability of computer code](#)

Data collection No software was used to collect data in this study.

Data analysis Code for developing the model and summarizing geospatial statistics in this study are available on GitHub at <https://github.com/wri/carbon-budget> and [https://github.com/wri/gfw\\_forest\\_loss\\_geotrellis](https://github.com/wri/gfw_forest_loss_geotrellis), respectively. Figure 2 was generated using R v3.5.0 and package ggplot2 v3.3.

For manuscripts utilizing custom algorithms or software that are central to the research but not yet described in published literature, software must be made available to editors and reviewers. We strongly encourage code deposition in a community repository (e.g. GitHub). See the Nature Research [guidelines for submitting code & software](#) for further information.

### Data

Policy information about [availability of data](#)

All manuscripts must include a [data availability statement](#). This statement should provide the following information, where applicable:

- Accession codes, unique identifiers, or web links for publicly available datasets
- A list of figures that have associated raw data
- A description of any restrictions on data availability

Geospatial data generated from the current study will be made publicly available on Global Forest Watch's Open Data Portal (<http://data.globalforestwatch.org/>) and from the corresponding author upon request. Summary geospatial statistics will be available from the Global Forest Watch dashboards and a publicly accessible API, as well as from the corresponding author upon request. All data analyzed as part of the current study are either publicly available or were obtained by the corresponding author upon request.

# Field-specific reporting

Please select the one below that is the best fit for your research. If you are not sure, read the appropriate sections before making your selection.

- Life sciences       Behavioural & social sciences       Ecological, evolutionary & environmental sciences

For a reference copy of the document with all sections, see [nature.com/documents/nr-reporting-summary-flat.pdf](https://nature.com/documents/nr-reporting-summary-flat.pdf)

## Ecological, evolutionary & environmental sciences study design

All studies must disclose on these points even when the disclosure is negative.

### Study description

The study design is structured as a geographic information system (GIS) model and is based on a synthesis of spatially explicit data sources to map gross and net greenhouse gas emissions and removals from global forest lands at 30-m resolution between 2001 and 2019.

### Research sample

Results of this study are not based on a statistical sampling design but on published wall-to-wall maps of global tree cover and tree cover change generated by Hansen et al. (2013) as well as other published geospatial data sets. The study area includes all global land except Antarctica and some small oceanic and Arctic islands. Table S3 documents the dozens of data sources we combined for this analysis. The model includes greenhouse gases CO<sub>2</sub>, CH<sub>4</sub>, and N<sub>2</sub>O, and six carbon pools.

### Sampling strategy

Results of this study are not based on a statistical sampling design, although quantification of uncertainty in this study is based in part on results from a probability-based stratified random sample of 1,500 blocks (120x120 m) to validate map-based estimates of global forest change. Three sub-strata were created per biome: no change, loss and gain. The sample allocation for each biome was 150 blocks for no change, 90 for change and 60 for gain (1,500 blocks total). For more information, refer to Hansen et al. (2013).

### Data collection

Results of this study are based on a synthesis of published datasets, not on original data collection. The datasets are combined using existing frameworks for calculating GHG emissions and removals (IPCC guidelines for national GHG inventory reporting).

### Timing and spatial scale

The time period of analysis covers 2001 to 2019. The starting and ending years were determined by the ranges of key data sources available during model development. The spatial scale of this study's results is 30-m resolution with full coverage of all continental land.

### Data exclusions

No data were excluded from this analysis.

### Reproducibility

The reproducibility of this study's results is facilitated by providing all model code used in a public repository (GitHub). Various data sources used as inputs into the study are publicly accessible and freely available.

### Randomization

This is not relevant to our study because results are not based on a statistical sampling design.

### Blinding

This is not relevant to our study because results are not generated based on a statistical sampling design.

Did the study involve field work?  Yes  No

## Reporting for specific materials, systems and methods

We require information from authors about some types of materials, experimental systems and methods used in many studies. Here, indicate whether each material, system or method listed is relevant to your study. If you are not sure if a list item applies to your research, read the appropriate section before selecting a response.

### Materials & experimental systems

- |     |   |
|-----|---|
| n/a | <input type="checkbox"/> Involved in the study<br><input checked="" type="checkbox"/> Antibodies<br><input checked="" type="checkbox"/> Eukaryotic cell lines<br><input checked="" type="checkbox"/> Palaeontology and archaeology<br><input checked="" type="checkbox"/> Animals and other organisms<br><input checked="" type="checkbox"/> Human research participants<br><input checked="" type="checkbox"/> Clinical data<br><input checked="" type="checkbox"/> Dual use research of concern |
|-----|---|

### Methods

- |     |  |
|-----|--|
| n/a | <input type="checkbox"/> Involved in the study<br><input checked="" type="checkbox"/> ChIP-seq<br><input checked="" type="checkbox"/> Flow cytometry<br><input checked="" type="checkbox"/> MRI-based neuroimaging |
|-----|--|